Cerebral Endothelial Function and Pulsatile Metaboreflex Hemodynamics in Adults

by

Luc Taylor

B.Sc., University of Victoria, 2021

A Thesis Submitted in Partial Fulfillment of the Requirements for the Degree of

MASTER OF SCIENCE

in the School of Exercise Science, Physical & Health Education

University of Victoria

We acknowledge and respect the Lək̓ʷəŋən (Songhees and Esquimalt) Peoples on whose territory the university stands, and the Lək̓ʷəŋən and W̱SÁNEĆ Peoples whose historical relationships with the land continue to this day.

Cerebral Endothelial Function and Pulsatile Metaboreflex Hemodynamics in Adults

by

Luc Taylor

B.Sc., University of Victoria, 2021

Supervisory Committee

Dr. Kurt Smith, Supervisor

School of Exercise Science, Physical & Health Education

Dr. Kirstin Lane, Academic Unit

School of Exercise Science, Physical & Health Education

Abstract

Few studies measuring cerebral blood flow (CBF) during metabolic afferent stimulation consider the mechanistic implications of endothelial function and compliance of vessels supplying the brain. The central question of this thesis study was whether pulsatile cerebral hemodynamic damping (DFi) plays a role in how the afferent muscle metaboreflex, a component of the exercise pressor reflex (EPR), impacts brain hemodynamics during exercise. Using ultrasound imaging techniques on 28 subjects (11 biological females, 17 biological males; 23.6±4.2 years of age; BMI of 24.0±3.2 kg/m^2), measures of DFi from the extracranial internal carotid artery (ICA) to the intracranial middle cerebral artery (MCA) were assessed during post-exercise muscle ischemia (PEMI) and transient hypercapnia (9% CO_2). Endothelial function was indexed by the %Δ in ICA vessel diameter (ICAd) during transient hypercapnia using a Douglas bag technique. DFi did not change during a paced-breathing metaboreflex stimulation; stimulation of the blood pressure-dependent metaboreflex with a 30% maximal voluntary contraction (MVC) dynamic handgrip protocol that preceded post-exercise muscle ischemia (PEMI) was effective (p = 0.005). A 6.77±3.97% increase in ICAd was observed during transient hypercapnia (p = 0.021). Cerebral hemodynamic buffering is maintained in healthy young male and female adults. Transient hypercapnia via Douglas bag provides an easy stimulus to increase $PetCO_2$ and shear stress to provoke ICA vasodilation. While no sex differences were observed in this study, future research could benefit from an increased sampling power to explore the impact of sex hormone levels. Additionally, considering healthy individuals appear to buffer cerebral hemodynamics, further mechanistic understanding is required to assess how aging and chronic disease-state populations lead to an impaired DFi.

Table of Contents

List of Figures

Chapter 2

Chapter 3

Chapter 4

List of Tables

Chapter 4

Appendix A

Glossary

ANOVA: Analysis of variance

AUC: Area under the curve

ATP: Adenosine triphosphate

BL: Baseline

BP: Blood pressure

CO_2: Carbon dioxide

CBF: Cerebral blood flow

CHEERS: Cerebrovascular Health Exercise and Environmental Research Sciences

CSV: Comma-separated value

CVC: Cerebrovascular conductance

CVR: Cerebrovascular resistance

DFi: Damping factor index

eNOS: Endothelial nitric oxide synthase

ECG: Electrocardiogram

EPR: Exercise pressor reflex

FMD: flow-mediated dilation

HR: Heart rate

ICA: Internal carotid artery

ICAd: Internal carotid artery diameter

ICAv: Internal carotid artery velocity

IQR: Inter-quartile range

MRI: Magnetic resonance imaging

MCA: Middle cerebral artery

MVC: Maximal voluntary contraction

NVC: Neurovascular coupling

O_2: Oxygen

PaO_2: Partial pressure of oxygen

$PaCO_2$: Partial pressure of arterial carbon dioxide

$PetCO_2$: Partial pressure of end-tidal carbon dioxide

PEMI: Post-exercise muscle ischemia

ROI: Region of interest

SMC: Smooth muscle cell

TCCD: Transcranial Color-Coded Doppler

TCD: Transcranial Doppler

VDu: Vascular Duplex

Acknowledgments

I am grateful for the opportunity to study under Dr. Kurt Smith during my graduate studies and extend this gratitude to the entirety of the Cerebrovascular Health Exercise and Environmental Research Sciences (CHEERS) Laboratory members who are insightful, dedicated, and supportive in the scientific research that we collectively perform.

When I began my university academic journey in Chemistry for the Medical Sciences at the undergraduate level, I had not expected such opportunity to perform health science research, though I have learned throughout these past two years that research in brain health measures is pertinent to many fields of human health sciences and is experimentally challenging, yet exciting.

As I continue onto professional academia, I bring with me the challenges overcome and lessons learned throughout my graduate studies in the School of Exercise, Physical & Health Education. The most valuable learning outcome for me is a honed ability to understand, critique, perform, and disseminate experimental scientific research; I feel as though these skills will be carried forth throughout my life, in aspects related and unrelated to academia. For that, I am grateful.

My final and special acknowledgment of gratitude is towards my family, who have supported my university academic journey since it began, with all of the tools that I needed to succeed in navigating this journey through undergraduate and graduate studies. These tools have not only carried me throughout my rearview journey but will continue to guide me ahead with purpose.

Chapter 1: Introduction

1.1 Theoretical Framework

Brain health is the state of brain functioning across cognitive, sensory, social-emotional, behavioural, and motor domains (World Health Organization, 2024). Regulation of brain health is largely linked to the maintenance of brain metabolism, which is dependent on brain blood flow and nutrient delivery. Both blood flow and nutrient delivery in the human brain depend on several physiological mechanisms: arterial blood pressure (BP), arterial blood gases, metabolism, and neural regulation synergistically serve to maintain adequate brain blood flow. Systemic regulation of metabolism during exercise stimulates cardiorespiratory (BP and ventilation) responses through neural reflexes responding to metabolically sensitive nerves in contracting skeletal muscle (Mitchell et al., 1983). The exercise pressor reflex (EPR) is a combination of chemical and mechanical reflexes that originate within contracting skeletal muscle and stimulate the systemic responses after being relayed through the brain through the spinal cord, with seminal research elucidating the BP regulation of this reflex nearly 100 years ago (Alam & Smirk, 1937). Until recently, the EPR and more specifically the metaboreflex (i.e., chemical reflex of the EPR), was thought to allow for the maintenance of flow and oxygen delivery to contracting muscle during exercise, by functionally increasing BP and heart rate (HR) (Fisher et al., 2015; Murphy et al., 2011). However, recent research suggests that the EPR does not facilitate flow and oxygen delivery to specific working muscles, but rather is crucial for establishing BP and autonomic regulation of non-active limbs during dynamic exercise (Thurston et al., 2023). Using an afferent spinal blockade (i.e., intrathecal fentanyl) during an EPR protocol, the researchers observed negligible muscle blood flow contribution by the EPR during large muscle post-exercise muscle ischemia (PEMI) and metabolic activation, compared

to an unblocked control condition. It remains to be seen how these results correspond with the blood flow and oxygen delivery to other organs in the body during metabolic afferent stimulation, such as the brain. Considering that metabolic activity in working muscles augments cerebral blood flow (CBF) regulation (Jorgensen, Perko, Hanel, et al., 1992), for the purpose of this thesis I aim to characterize the mechanistic regulation of cerebral hemodynamics during metaboreflex stimulation. The significance of this inquiry is to develop an important understanding of the metabolic regulatory component in regulating CBF during exercise.

In the brain, the ability to buffer the BP increase whilst maintaining adequate flow may be a product of EPR activation during exercise, though this requires further mechanistic insight; regional flow velocity increases have been shown to occur when stimulating the EPR (Ogoh et al., 2019; Prodel et al., 2016). Recent research supports the notion that CBF may be largely unaffected by cerebral sympathetic activity when stimulating the EPR (Tymko et al., 2024). Regardless of the volumetric changes in blood flow to the brain during an EPR test, what may be more interesting to determine is if the EPR facilitates the attenuation of deleterious hemodynamic forces through the brain caused by the increase in systemic pressure. This is possible by assessing pulsatile hemodynamic decompensation (i.e., damping) as it travels in a proximal to distal direction through extracranial to intracranial cerebral vessels. The damping of the pulse pressure and flow from outside of the cranium to inside the cranium provides an index of cerebrovascular stiffness/compliance and is an important marker of cerebrovascular function with normal aging (Lefferts et al., 2021). Thus, mechanistic insight into how exercise interacts with the brain's blood flow maintenance mechanisms is an important area of research.

This thesis is primarily focused on characterizing the cerebral vasomotor responses to neuromuscular stimulation during fatiguing handgrip exercise, and quantifying if cerebral

endothelial function may be associated with these responses. The resultant goal was to assess and observe if brain blood flow responses to metabolic stimulation (i.e., EPR) are related to the brain's ability to buffer hemodynamic stresses during exercise and ischemia promotion in young adults aged 19-35 years, using a cross-sectional design. The muscle metaboreflex in peripheral cardiovascular systems is understood to integrate with central brain-stem areas that are signaled when muscle metabolites build up during fatiguing exercise, which feedback into the cardiovascular system (i.e., metabolic reflexes). It is not known whether these signals stimulate changes in blood vessel diameter and resultant blood flow, or the ability for the brain to attenuate hemodynamic stresses.

Additionally, measures of endothelial function in relation to the hemodynamic changes during muscle metaboreflex stimulation are not well defined, considering that no study has specifically investigated this. However, the degree to which cerebral endothelial function influences hemodynamics during metabolic stimulation may help to understand if there is a link between the compliance of the extracranial to intracranial vasculature during exercise. Alterations in blood gas concentrations (i.e., O_2 and CO_2) from ventilatory changes during EPR stimulation may trigger intracranial vasoconstriction given EPR induces hypocapnia (Braz et al., 2014; Prodel et al., 2016). During handgrip, a collective MCA vasoconstriction has been observed using magnetic resonance imaging (MRI), however individual responses indicated significant inter-participant variability (Verbree et al., 2017). The degree of hypo- and hypercapnia on cerebrovascular responses to dynamic whole-body exercise have previously been observed (Moraine et al., 1993; Smith et al., 2014); during whole-body exercise, mechanical sheer stress has been suggested to stimulate endothelial cells and induce vasodilatory responses (Ogoh & Ainslie, 2009; Smith et al., 2019). It remains to be investigated if endothelial function

influences cerebrovascular metaboreflex responses, however, it is likely that CO_2 sensitivities may impact how the brain regulates hemodynamics during exercise. Less compliant vessels that do not vasodilate in response to hypercapnia or metabolic stimulation are likely to have a greater transmittance of pressure to the microvasculature in the brain. Understanding the mechanisms that influence CBF regulation is important in characterizing brain health, as consistent bombardment of the brain's vasculature with higher pressure transmittance (i.e., less damping) over the adult lifespan has been linked with greater cerebral artery aging and cognitive decline (Toth et al., 2017).

Chapter 2: Literature Review

2.1 Reflexive Hemodynamic Control Mechanisms During Exercise

Within historical literature, BP responses to fatiguing exercise are dependent on reflexive responses to metabolic substance production and utilization (Alam & Smirk, 1937). The substances have since been identified as the following known metabolites produced by skeletal muscles during fatiguing exercise: lactic acid (lactate and protons), arachidonic acid (Rotto & Kaufman, 1988; Rotto et al., 1989), adenosine (Costa & Biaggioni, 1994), bradykinin (Stebbins & Longhurst, 1985), diprotonated phosphate (Gao et al., 2006; Sinoway et al., 1994), adenosine triphosphate (ATP) analogues (Li et al., 2008) and potassium (Kniffki et al., 1978; Rybicki et al., 1984). This reception of these metabolites appears to be biochemically distinct between group IV afferent subtypes (Amann et al., 2015), though the metabolites produced during fatiguing exercise appear to integrate similarly to a collective cardiorespiratory response when group IV afferent signalling is relayed through the brainstem areas, modulating BP and autonomic outflows. The robust cardiorespiratory response to EPR is a summation of all of the group IV afferent subtypes; however, it is beyond the scope of this thesis to ascertain the individual contribution of these subtypes to the EPR.

While the metaboreflex does not appear to alter cerebral sympathetic activity, increases in muscle sympathetic nerve activity (MSNA) corroborate the systemic metaboreflex responses (Fisher et al., 2013). However, pertinent contradictions to the increased MSNA during metaboreflex stimulation have been observed, in which only the non-contracting muscles (i.e., opposite limb) were observed to have an increase in MSNA following metaboreflex stimulation (Boulton et al., 2018). The researchers suggest that the mechanoreception (i.e., group III afferents) in the lower limb governs changes in MSNA of contracting muscles during isometric

exercise and proceeding ischemia instead of the metabosensitive afferents. This response is likely exercise mode and limb-dependent (Boushel, 2010). Regardless if MSNA is influenced by the metaboreflex in contracting muscle or not, the effects of metaboreflex activation are not limited to BP and MSNA modulation, inducing several cardiovascular responses such as hyperventilation (Amann et al., 2011; Laginestra et al., 2023), cardiac output (Ogoh, 2024), and/or cerebrovascular vascular resistance (CVR) (Lis et al., 2021; Nobrega et al., 2014) that influence CBF regulation. These responses, in relation to other mechanisms of cardiovascular adjustments during exercise, are integrative and make isolating the metaboreflex challenging; other additive mechanisms occurring during exercise include the muscle mechanoreflex, baroreflex, chemoreflex, and central (efferent) command control, which together define the cardiovascular state during exercise (Lambert, 2005; Lis et al., 2021).

2.1.1 Isolating the Muscle Metaboreflex

The PEMI methodology is designed to isolate the metaboreflex; it is also referred to in the literature as post-exercise circulatory occlusion (PECO) or post-exercise circulatory arrest (PECA), but will be henceforth referred to as PEMI. Despite differences in terminology, each technique relies on assessing cardiorespiratory responses to a group of exercising muscles, during the exercise and following rapid circulatory arrest of the exercising limb blood flow from the systemic circulation. This circulatory arrest preserves the metabolic stimulus, while also removing the confounds of descending neurogenic command/responses (Delaney et al., 2010; Ng et al., 1994). Promotion of ischemia is integral to the understanding of sustained BP and MSNA activation during and after exercise, due to metabolically sensitive afferent fibres. It is suggested that MSNA activation due to exercise and PEMI does not have a significant correlation with

aging in adulthood (Ng et al., 1994), and the BP elevation may be more significant in hypertensive populations (Sausen et al., 2009). How the metaboreflex impacts cerebral hemodynamics is not wholly developed, as it is unclear if (1) the cerebral vasculature vasodilates or vasoconstricts in response to the metaboreflex and (2) if pulsatile hemodynamic forces are buffered or transmitted.

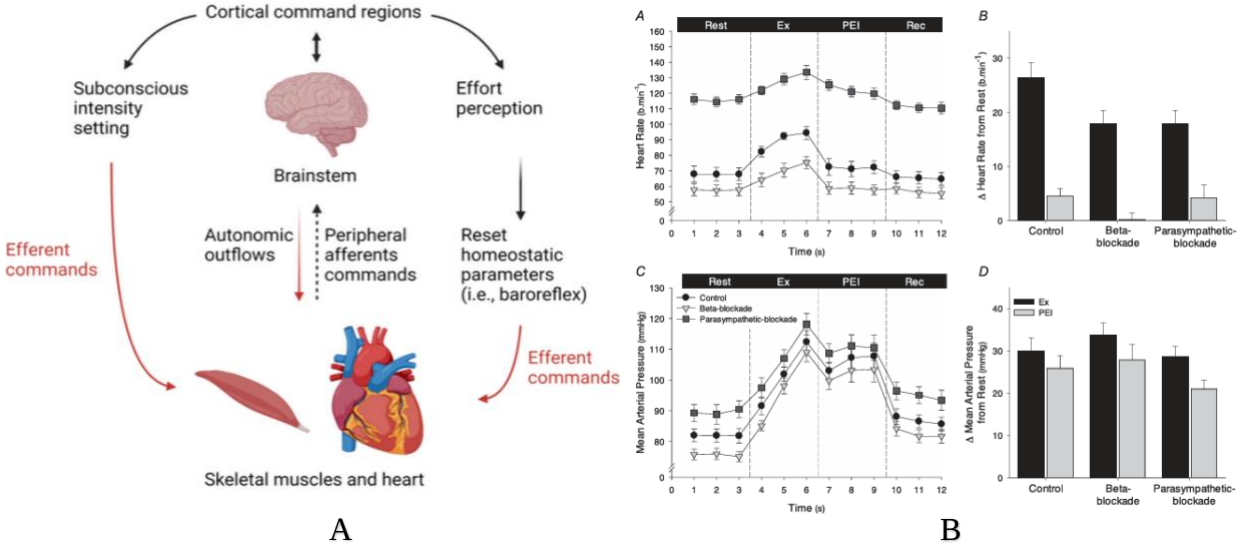

Figure 2.1. (A) Schematic of peripheral efferent commands (red) in relation to the autonomic control and central processing that ultimately modulate output during exercise (Lambert, 2005; Nobrega et al., 2014). Created with BioRender.com. (B) Adapted figure from Fisher et al. (2013) demonstrating the use of post-exercise muscle ischemia (PEMI) following handgrip exercise (Ex), in terms of mean arterial pressure (MAP) and heart rate (HR) with and without sympathetic (▽) or parasympathetic (■) blockades compared to control (●). The bar graphs in this figure (*B* and *D*) depict the change from rest in both cardiorespiratory parameters, during handgrip exercise PEMI/PEI.

The metaboreflex has an integral role in the EPR, representing one of the two reflexes in terms of mechanistic value; the mechanoreflex integrates with the metaboreflex to form the EPR. Overall, the EPR is understood to induce changes in BP and HR during exercise, reflexively (Fisher et al., 2015; O'Leary, 1993). Differing from the metaboreflex, the mechanoreflex involves stimulation of group III afferent fibres via the fatiguing mechanical contraction of skeletal muscle and elicits similar isolated hemodynamic changes compared with the

metaboreflex, when proper methodological considerations are in place (Drew et al., 2008; Fisher et al., 2005). Although the afferent components of the EPR are mechanistically individual, there is a hyperadditive effect of the mechano- and metaboreflex; pre-activation of metabosensitive afferents (i.e., group IV) is associated with greater activation of mechanoreflex-mediated HR and ventilatory responses (Drew et al., 2008; Laginestra et al., 2023). The role of group III and IV afferents has been shown to be important in determining the exercise intolerance of cardiovascular disease-state populations, specifically heart failure patients (Amann et al., 2014). The EPR is associated with preventing premature fatigue in populations with normal cardiovascular function, however, the negative feedback towards tolerance of fatigue during exercise means that optimization of muscular endurance during exercise is balancing both efferent and afferent activation (Amann et al., 2011).

2.1.2 Integration of the Baroreflex, Chemoreflex, Central Command, and EPR

Another mechanism, the baroreflex, employs baroreceptor activation primarily within the walls of the aorta and carotid sinus, resulting in decreased HR during states of elevated BP; the metaboreflex can functionally "reset" the baroreflex activation window (Figure 2.2), thus higher BP is able to be sustained during exercise without HR modulation and downstream decreases in flow (Dipla et al., 2013; Raven, 2008). The baroreflex is not a focus of this thesis and has been mechanistically reviewed elsewhere (Lanfranchi & Somers, 2002). Another feedback mechanism, the chemoreflex, has both peripheral (i.e., carotid arteries, aorta, pulmonary arteries, and veins) and central (i.e., medullary) components, which respond to arterial oxygen (O_2) concentrations and neural CO_2 concentrations, respectively (Wan et al., 2020). As a result of exercise-induced partial pressure of O_2 (PaO_2) decrease, the chemoreflex response modulates

ventilatory frequency and thus end-tidal gas concentrations to maintain adequate oxygenation in the working muscle; this has been shown to have a hyperadditive effect with the EPR in relation to BP and HR (Wan et al., 2020). As with the baroreflex, this mechanism gives context to the EPR in terms of cardiorespiratory modulation but is not a focus of this thesis and has been reviewed in detail elsewhere (Guyenet, 2014). The central command represents cortical regions that define afferent commands to muscles, which input the cardiovascular and respiratory control during exercise, influencing muscle activation and downstream effects of neurogenic reflexes (Goodwin et al., 1972); a detailed mechanistic review of the central command has been published elsewhere (Nobrega et al., 2014; Williamson, 2010). As aforementioned, the complication of the hemodynamic reflexes in response to exercise is apparent. Discussion of exercise-related mechanisms of brain blood flow regulation rarely focus on these hemodynamic reflexes, yet the individual peripheral and central control mechanisms have regulatory outcomes that likely determine CBF parameters during exercise.

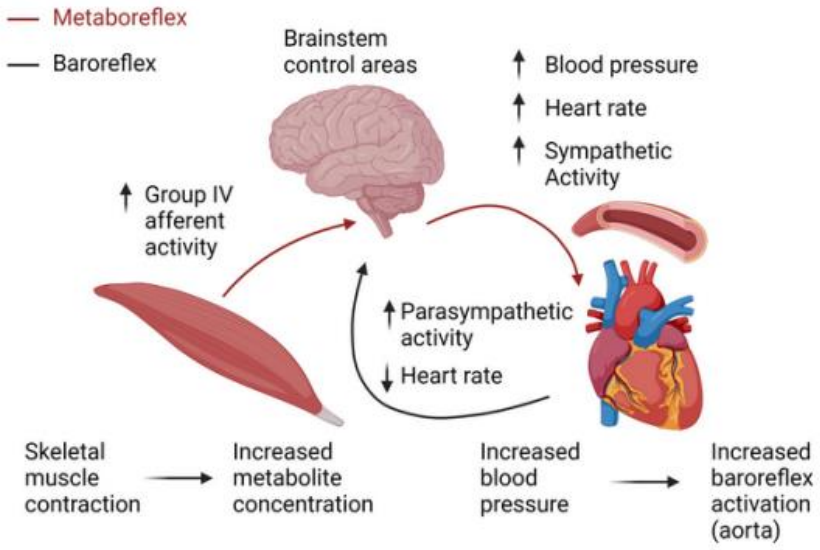

Figure 2.2. Integration of the muscle metaboreflex with the baroreflex in terms of hemodynamic parameters during exercise (Ichinose et al., 2008; O'Leary, 1993). Created with BioRender.com.

2.1.3 Cerebrovascular Flow Implications of the Metaboreflex

The first assessment of cerebrovascular-related effects of the EPR was done in 1992, in which the researchers used dynamic exercise and a separate single-arm fatiguing exercise protocol to probe the changes in CBF (Jorgensen, Perko, Hanel, et al., 1992). This publication references the observations that average or total CBF appears constant during exercise, however, cortical or regional changes in CBF may be significant during exercise. The researchers' later work supported the increase in regional CBF, observed in the middle cerebral artery (MCA) on the contralateral side of the exercising limb only when afferent signals were intact (Jorgensen et al., 1993), using transcranial Doppler (TCD) ultrasonography techniques to measure mean arterial flow velocity. Observations as such are typically measured with TCD, transcranial color-coded Doppler (TCCD), or MRI techniques. Likely, these findings were observed due to accounting for ventilatory changes in the partial pressure of arterial CO_2 ($PaCO_2$), or the surrogate measure of the partial pressure of end-tidal CO_2 ($PetCO_2$), as the researchers denote that decreases in $PaCO_2$ may not reflect the absolute increase in blood flow velocity (Jorgensen et al., 1993). They support the longstanding notion that changes in CBF are tightly correlated to changes in $PaCO_2$ (Reivich, 1964); by controlling for ventilation during exercise, such as by standardizing breathing rate, more accurate observations of specific mechanistic changes in cerebral hemodynamics were possible. Thus, future studies investigating the metaboreflex need to consider how changes in CO_2 influence the cerebrovascular response.

As with peripherally focused cardiovascular research, PEMI is a viable modality of assessing the response of cerebral arteries to exercise and metabolic stimulus. During dynamic exercise, the mean arterial flow velocity of cerebral arteries, namely the MCA and internal carotid artery (ICA) is increased, primarily as a function of HR and BP elevation (Gonzalez-Alonso et al.,

2004; Hellstrom & Wahlgren, 1993; Jorgensen, Perko, & Secher, 1992; Moraine et al., 1993; Washio et al., 2021). Post-exercise, the promotion of ischemia causes increased blood flow in the MCA and ICA compared to rest, independent of central command (Jorgensen, Perko, Hanel, et al., 1992; Ogoh et al., 2019; Prodel et al., 2016) and independently of increases in MSNA caused by the metaboreflex (Pott et al., 1997). Cerebral hemodynamic changes may be unique during and after exercise in terms of the metaboreflex, as non-cerebral arteries have not demonstrated the same change in flow (Ogoh et al., 2019); this challenges the nature of the current research field to assess cerebral hemodynamic changes to the metaboreflex, specifically and reproducibly.

To accurately assess the cerebrovascular implications of the sustained metabosensitive afferent activation, studies need to control for ventilation during PEMI; this is due to changes in $PaCO_2$ causing downstream endothelial responses which alter flow rates, irrespective of efferent command (Braz et al., 2014; Prodel et al., 2016). Because CBF is a product of diameter and velocity, with diameter having a more pronounced role, previous conclusions regarding the influence of the metaboreflex and exercise on CBF could be misleading. As such, valid measures of CBF require the assessment of concurrent velocity and diameter, and not simply assuming constant arterial diameter, while also understanding hemodynamic changes. Observations of decreased MCA diameter have been associated with dynamic handgrip exercise at isocapnia (Verbree et al., 2017). This observed decrease in vessel diameter was suggested to be explained by an increase in cerebral sympathetic activation, though recently published data suggests that cerebral sympathetic activity does not increase during isometric exercise or during PEMI when CO_2 is maintained using end-tidal forcing (Tymko et al., 2024). These competing observations may be explained by the differential intensity and mode of the handgrip exercise (i.e., 30% maximal voluntary contraction [MVC] and dynamic, versus 60% MVC and isometric), though

dynamic cycling exercise showed a similar lack of cerebral sympathetic activation (Tymko et al., 2024); in any case, the changes in hemodynamic control during handgrip exercise and PEMI illustrate how the metaboreflex may help the brain respond to hemodynamic stress when evaluating PEMI responses with corresponding endothelial function.

2.2 Cerebral Endothelial Function

Endothelial function is characterized by the vasodilatory capability of a vessel in response to a mechanical shear stress stimulus and is a pertinent measure of vascular health, as endothelial dysfunction is associated with vascular disease risk in peripheral (Green et al., 2011; Ras et al., 2013) and cerebral (Toda, 2012) vasculatures. Vasodilation can be signalled directly through chemical biomarkers that induce vascular smooth muscle cell (SMC) relaxation, such as nitric oxide (NO) and its precursors (Ratchford et al., 2022; Trinity et al., 2016), or in cerebral vasculature through hypercapnia (i.e., increased $PaCO_2$); NO and hypercapnic vasodilatory signals are stimulated by increases in mechanical shear stress in cerebral arteries (Carter et al., 2016; Hoiland et al., 2022; Hoiland et al., 2018). An increase in blood flow and flow velocity have local effects on increasing shear stress through a vessel, which has long been associated with activating the endothelial nitric oxide synthase (eNOS) pathway for vasodilation via phosphorylation (Fisslthaler et al., 2000; Pohl et al., 1986; Rubanyi et al., 1986). Measures of endothelial function often assess peripheral artery changes during a vasodilatory stimulus, such as using ultrasound measures during reactive hyperemia (i.e., flow-mediated dilation [FMD]) (Sinoway et al., 1989; Thijssen et al., 2011; Thijssen et al., 2019); this technique is sufficiently sensitive and reproducible for assessing the vasodilatory capacity of vessels, and thus has

implications for relating endothelial functional differences to the risk atherosclerosis and heart disease in humans (Anderson et al., 1995; Charakida et al., 2010; Nabel et al., 1990).

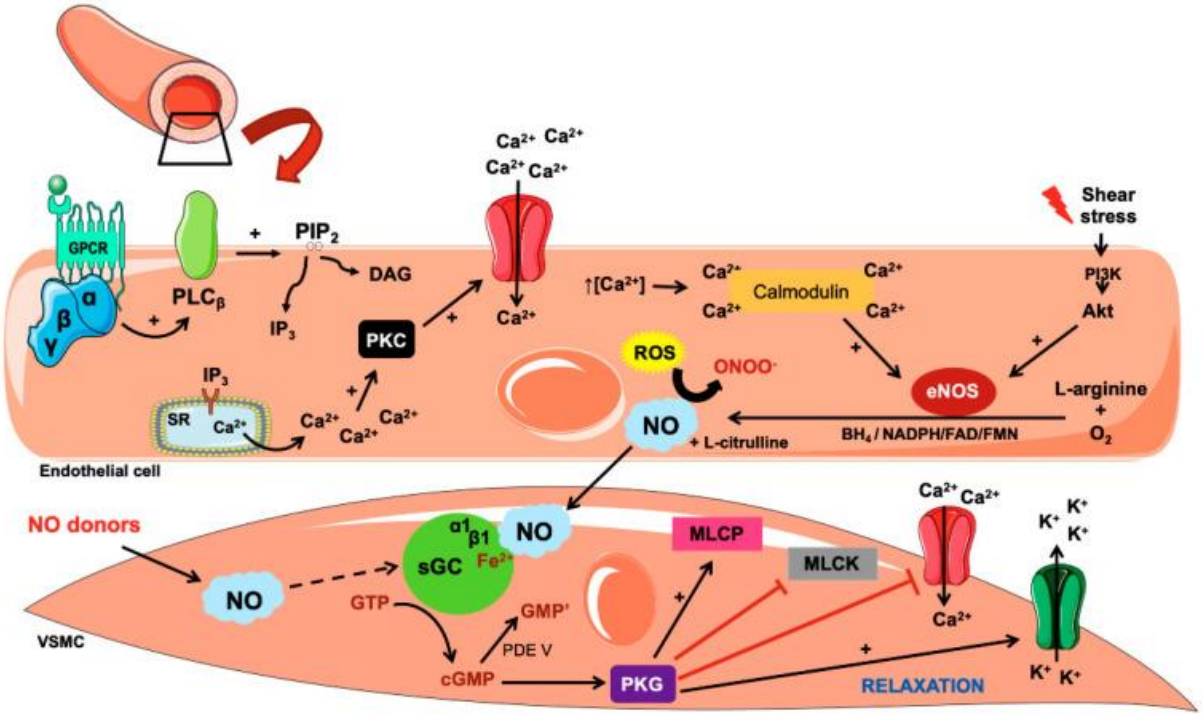

Figure 2.3. Adapted schematic from da Silva et al. (2021) demonstrating the shear-mediated endothelial nitric oxide synthase (eNOS) activation pathway, in the vessel endothelium; nitric oxide (NO) production and stimulation of vascular smooth muscle cell (SMC) relaxation is further depicted as a product of the endothelial function.

As aforementioned, proper regulation of CBF through a complex vasculature in the brain provides synergistic and redundant protection of brain health; the interactions of arterial BP, blood gases, and neurogenic regulations help facilitate the matching of perfusion to neuronal metabolic demand (Claassen et al., 2021; Mavroudis et al., 2022). The brain is a highly metabolically active organ and requires consistent levels of blood perfusion to meet metabolic (Claassen et al., 2021; Magistretti & Allaman, 2015). In order to achieve proper CBF regulation, endothelial function must be intact; however, the ability to relate peripheral endothelial function to cerebral measures is unclear, due to an observed lack of relationship between peripheral and cerebral endothelial function in young, healthy adults (Carr et al., 2020). That said, a positive

relationship between peripheral endothelial dysfunction and cerebrovascular disease has been observed in people with preexisting Parkinson's disease (Yoon et al., 2014). In any case, the functional stimulation of the endothelium via increasing shear stress and thus eNOS activation is relevant for both measures of peripheral and cerebral endothelial function, given the reliance on this pathway regardless of conduit vessel location.

Stimulating endothelium-dependent vasodilation via shear stress in conduit brain arteries requires different methodological considerations to that of peripheral artery measures (e.g., brachial) (Carr et al., 2020). A novel method of promoting shear-mediated vasodilation in the brain is by measuring cerebral vasomotor responses to a transient hypercapnic stimulus. This stimulus may be beneficial to characterize cerebral hemodynamic adaptation during PEMI, as the aforementioned tight control of CBF with $PaCO_2$ and a unique impact of PEMI on cerebral vasculature may illustrate how endothelial function informs exercise-dependent hemodynamic changes.

2.3 Pulsatile Hemodynamic Damping

Stiffening of an arterial vessel will impede BP-mediated vascular adjustments that aim to optimize flow waveforms (Reymond et al., 2012). Stiff arteries impede vascular hemodynamics by altering arterial compliance, which is defined as the act of a conduit artery storing waveform energy by stretching each cardiac cycle. Healthy arterial compliance attenuates harmful pulsatile waveforms (i.e., high force transmittance) and maintains blood flow while reducing the severity of pulsatile forces along macro- to microvascular environments. This is important considering that microvascular environments are vulnerable to higher pulsatile forces, and transmission rather than buffering of these forces may result in vascular dysfunction at the level of the organ.

Thus, the term compliance describes the inherent ability of a conduit vessel to buffer changes in arterial BP. Damping is a term that can be applied to a conduit vessel with an expected degree of compliance. The compliance (i.e., pulsatile hemodynamic buffering) of these vessels influenced by the vascular structure, tortuosity, and functional stiffness can be indexed by quantifying the change in pulsatility (PI) along proximal to distal arterial segments, which is referred to as damping (Lefferts et al., 2021). Empirical calculations of damping from extracranial to intracranial arteries are represented using the damping factor index (DFi); the DFi represents relative PI between proximal to distal conduits vessels and is an important marker of downstream cerebrovascular function, yet remains mechanistically underdefined (Lefferts et al., 2020; Pan et al., 2022). Increases in arterial stiffening are directly associated with decreased arterial compliance, as the conduit vessel is less capable of structural hemodynamic adaptations, and thus is less compliant. Compliance relates to cerebrovascular function as the ability of conduit vessels to alter their structure to accommodate changes in flow is related to the delivery of hemodynamic forces to the downstream microvessels, which perfuse brain tissue. The PI of a conduit vessel is defined by the systolic and diastolic velocities relative to the mean velocity for that vessel, meaning that PI is related to the structural arterial compliance of a vessel during each cardiac cycle (Lefferts et al., 2020; Thomas et al., 2021). It is worth mentioning that damping differs also from compliance as it encompasses blood vessel compliance, structural changes in tortuosity, as well as downstream cerebrovascular conductance (CVC) and CVR.

2.4 Cerebral Autoregulation and CO_2 Reactivity – A PEMI Perspective

The synergistic impact of arterial BP regulation and CO_2 reactivity on CBF results in hypo- and hypercapnia having blunting and enhancing cerebral pressure perfusion relationships.

Throughout this thesis, the BP and $PaCO_2$ synergisms are hypothesized to provide functional hemodynamic protection during acute stressors. Cerebral autoregulation is a descriptor of the cerebral vasculature to maintain consistent flow parameters, irrespective of changes in BP (i.e., cerebral perfusion pressure); CO_2 reactivity correlates to cerebral autoregulation in that changes in $PaCO_2$ induce a change in arterial diameter. For example, increases in $PaCO_2$ induce increases in arterial diameter and decreases in CVR, further inducing an increase in CBF that may be damaging to microvasculature if not attenuated by normal cerebral autoregulation (Ainslie et al., 2007). The intersection of cerebrovascular reactivity to CO_2 and cerebral autoregulation serves to maintain normal cerebral perfusion pressure during states of increased $PaCO_2$ or MAP; the quantification of cerebral autoregulation is not accounted for in this thesis, however, it is important to recognize the impact that this mechanism has with dynamic BP challenges (Brassard et al., 2023). Impairment of shear-mediated vasodilation may be caused by decreases in cerebrovascular reactivity to CO_2; along with inferred reductions in cerebral autoregulation, this may infer an increased subspecialty to cerebrovascular events (i.e., stroke) due to a higher pulsatile pressure transmittance to microvasculature in the brain (Ainslie et al., 2007).

In terms of detrimental pulsatile transmittance, the ability of the brain's vasculature to accommodate changes in MAP (e.g., static or dynamic) appears to become attenuated when the $PaCO_2$ increases (Ainslie et al., 2005; Perry et al., 2014), which is paradoxical to the ability of the brain to maintain normal perfusion pressure during times of higher $PaCO_2$ or MAP. This accentuates the idea that controlling for changes in $PaCO_2$ to some degree, while also having some measure of CO_2 reactivity, may be important in elucidating how the BP stressor of the metaboreflex impacts cerebral hemodynamics.

2.5 Purpose and Hypothesis

Given the provided literature review, this thesis describes the current state of knowledge for the mechanisms underlying cerebral hemodynamic regulation during metaboreflex stimulation. With proper context for historic PEMI investigations compared to more modern assessments of hemodynamics when probing the metaboreflex, the gap in knowledge is elucidated regarding how the brain responds to exercise-dependent mechanisms. Existing measures of CBF responses to PEMI stimulation disregard the mechanistic implications of endothelial function and compliance of large vessels that feed the brain; whether pulsatile damping, which is inherently related to the functional stiffness of these vessels, plays a role in understanding how the metaboreflex impacts brain hemodynamics during exercise, is central to this thesis.

2.5.1 Purpose

The purpose of this study was to (1) quantify CBF regulation and hemodynamic responses to metaboreflex stimulation, as well as to increased arterial shear stress. The shear stress stimulus was intended to reflect the cerebral endothelial function as a measure of changes in ICA diameter. Additionally, this study set out to determine if (2) the metaboreflex hemodynamic responses are associated with the cerebral endothelial function responses, given the probable influence of CO_2 reactivity during metaboreflex stimulation. Comparing these factors in adults provides a novel characterization of vascular properties responsible for healthy CBF regulation during exercise. Thus, the primary objective of this study was to assess CBF regulation at rest, during and immediately following a single-limb dynamic fatiguing handgrip exercise to isolate the metaboreflex, as well as during a 30-second hypercapnic breathing challenge.

2.5.2 Hypothesis

Our hypothesis was that (1) the cerebrovascular hemodynamic damping at rest would be preserved during handgrip exercise and subsequent PEMI. Because of CO_2 reactivity responses highlighted during PEMI, we also hypothesized that (2) the endothelial response (i.e., degree of vasodilation) to transient CO_2 would be positively correlated to the hemodynamic buffering observed during exercise and metaboreflex stimulation (i.e., handgrip and PEMI).

Chapter 3: Methodology

3.1 Registration and Recruitment

This study received ethical approval from the University of Victoria's Human Research Ethics Board on November 1, 2023 (protocol #23-0140); young and generally healthy adults aged 19-35 years were recruited by self-registration. Recruitment was primarily done at the University of Victoria via noticeboard posters and class presentations, additionally with snowball sampling and social media post promotion. Upon correspondence with Luc Taylor, all screening and testing sessions were scheduled and performed at the University of Victoria's McKinnon Building.

3.1.1 Eligibility Criteria

To participate in this thesis study, individuals must have completed a health and background screening questionnaire, reporting that they were generally healthy with no underlying self-reported chronic diseases, such as a history or diagnosis of heart disease, anemia, high BP, respiratory disease (i.e., including asthma), stroke, kidney disease, diabetes, myocarditis, panic/anxiety disorders, or any disorder identified to potentially confound healthy cerebrovascular aging. Participants must have also been able to physically perform handgrip exercise, have a BP cuff administered to them, and breathe through the cardiorespiratory breathing device (i.e., mouthpiece and tube). This study did not include individuals who are addicted smokers (i.e., report dependence and withdrawal symptoms from using vapes, cigarettes, e-cigarettes, and marijuana) or who had a medical professional advise them to avoid exercise.

Any of the above conditions or characteristics would have significantly altered the variables and cerebrovascular responses that were measured in ways that would not accurately represent healthy young people, while also compromising the well-being of more at-risk individuals. Individuals who did not identify with the sex they were assigned at birth were not restricted from this research; participants were asked to report their assigned sex at birth on the screening questionnaire, no matter their gender identification or use of hormone suppression pharmacotherapy, as all participants' results were stratified based on their biological sex to assess sex differences as a tertiary outcome. Along with the general health and background screening form, all participants completed a PAR-Q+ form to confirm their ability to perform the exercise within the protocol; any contraindication to exercising based on this questionnaire resulted in the possible participant not being included in any of the study protocols.

3.1.2 Pre-Screening

A pre-screening resting BP measure was taken at the brachium, using an automatic BP monitor (BIOS Diagnostics 3MS1-4Y, BIOS Diagnostics, ON, CA). If this BP reading was under 160/90 mmHg, the participant was eligible to continue with the study protocol; this upper limit for exercise-related testing is consistent with the updated recommendations per the Canadian Society for Exercise Physiology (CSEP) guidelines (CSEP, 2021). Participants were asked not to take any pain medications (e.g., ibuprofen, opioids) within six hours of the test; during the day of testing, each participant was asked to report if they took any medications on that day, to better account for drug-related variances. Additionally, participants had their testing visits rescheduled if they (1) performed moderate to vigorous intensity exercise within 24 hours of their scheduled testing session, (2) had alcohol or caffeine within 12 hours of their scheduled

testing session, or (3) had eaten within six hours of their scheduled testing session, as to not further confound the hemodynamic measures in this study.

Pre-screening for vessel imaging quality in ultrasound was done to ensure that the MCA and ICA were accessible and resolved for accurate ultrasound measurements. Maximal grip strength of the measured limb was assessed using a digital hand grip dynamometer (BIOPAC MP3X, BIOPAC Systems, CA, USA) before the measurement protocol, using the greatest score of two attempts to calculate MVC. This initial test of maximal contraction force was used to calculate the 30% MVC used in the study data.

3.2 Procedure and Protocols

While the participant was in a supine position, assessments of intracranial (i.e., MCA) and extracranial (i.e., ICA) cerebral vessels were performed at rest, during a transient CO_2 breathing test, and during submaximal hand grip exercise (30% of MVC) with subsequent occlusion to promote muscle ischemia, using a non-diagnostic TCCD ultrasound for MCA measures (Vivid Q, GE Healthcare, IL, USA) and a vascular Duplex (Vdu) ultrasound for ICA measures (Terason 3300, Teratech Corporation, MA, USA).

3.2.1 Ultrasound Instrumentation

Although MRI is commonly adopted for usage in diagnostic brain health given its high spatial resolution, its lower temporal resolution limits its use in measuring dynamic cerebrovascular function. In contrast, Doppler ultrasound provides continuous high temporal and spatial resolution quantification of intracranial and extracranial cerebrovascular hemodynamics and thus TCCD and VDu ultrasound were deemed the most appropriate modalities to measure brain

hemodynamics in this thesis study. These ultrasound techniques rely on soundwaves that propagate through tissue and reflect off of the flowing blood through conduit vessels (Aaslid et al., 1982); the velocity of blood can therein be measured, given the adjustment for the angle of intonation and ultrasound probe frequency (i.e., piezoelectric crystal) (Oglat et al., 2018). For this study, the ultrasound information was captured using an angle of insonation between 0-60° and a probe frequency of 2 MHz and 10 MHz for TCCD and VDu, respectively. Given the soft tissue depth for VDu compared to TCCD, along with the higher probe frequency and ability for concurrent real-time cross-sectional area imaging with velocity waveforms, only the VDu (Terason 3300, Teratech Corporation, MA, USA) allowed for accurate CBF quantification in this study.

The ultrasound probes interfaced with a portable computer that allows for measuring cerebral hemodynamics. To obtain an image of the ultrasound signal in both modalities, the sound information is processed into a video output by the respective ultrasound's portable computer, captured using offline video collection software (Camtasia, TechSmith, MI, USA). Using the portable VDu, the diameter of the ICA was imaged in B-mode, while simultaneously capturing flow velocity in pulse-wave mode; no alterations of B-mode settings were made after the resting baseline acquisition (BL), to avoid any artificial changes in arterial wall brightness/thickness. The VDu probe was placed on the anterolateral aspect of the neck with some petroleum gel, to landmark the correct insonation window and image the ICA. Measurements were taken >1.5 cm distal to the common carotid bifurcation to eliminate recordings of turbulent and retrograde flow, holding the sample volume parallel to the vessel walls (<60 degrees) in the middle of the vessel to optimize the recording of laminar flow, as outlined by Thomas et al. (2015).

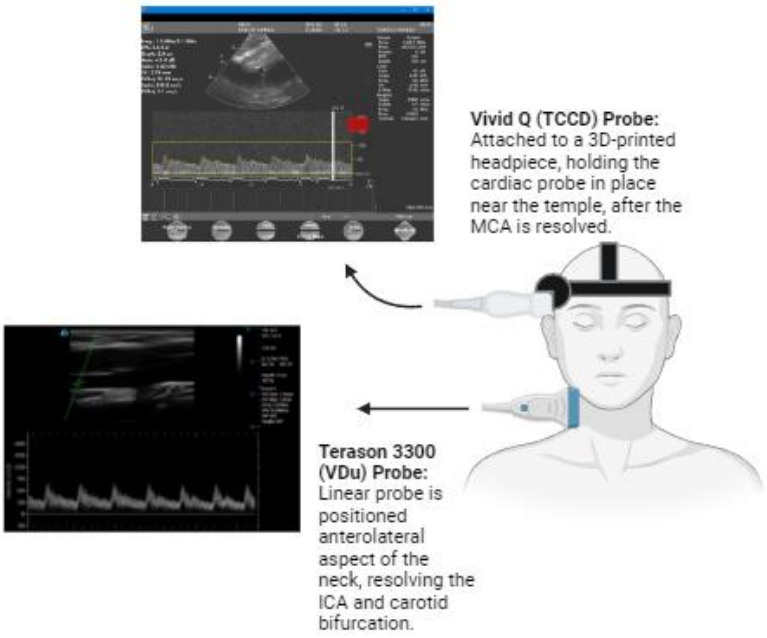

Figure 3.1. Schematic of the ultrasound instrumentation, illustrating the placement of transcranial color-coded Doppler (TCCD) and vascular duplex (VDu) ultrasound probes and their respective outputs to the portable computers, to image blood velocity and/or vessel diameter. Created with BioRender.com.

Measurements for the MCA were performed by attaching the TCCD probe to a head frame, making it possible to hold the probe within the insonation window, then placing the probe and some petroleum imaging gel near the temple to image the MCA. The imaged segment of the MCA was chosen based off of pilot testing results, wherein the longest and least digitally noisy segment available was angle-corrected and assessed. Initial search and selection criteria followed TCD guidelines defined previously by Willie et al. (2011), while optimization for the highest ICA velocity based on the VDu angle criteria was performed as outlined by Thomas et al. (Thomas et al., 2015). Additionally, the electrical activity of the heart was assessed concurrently with the TCCD imaging using a 3-lead ECG, placed on the torso using Einthoven's triangular landmarks (Einthoven, 1912; Salam, 2019). The ECG signal was delivered into the ultrasound machine, which further interfaced with a computer; this computer also received signals from a

digital collection box (Bioamp, ADInstruments, CO, USA) that calculates HR and BP continuously by using photoplethysmography monitoring (hNIBP Nano, ADInstruments, CO, USA), which the computer processed into a digital acquisition software (LabChart, ADInstruments, CO, USA).

3.2.2 Assessment of Endothelial Function – the Breathing Protocol

For the hypercapnic breathing protocol, a 100 L Douglas bag, a medical-grade reservoir filled with specific concentrations of atmospheric respiratory gases (9% CO_2, 20.97% O_2, and balanced nitrogen); notably, this Douglas bag contained a super-atmospheric level of CO_2 (~0.04% in the atmosphere). Given that the level of CO_2 was higher in the bag than in the atmosphere, breathing through the mixed gas from this bag increased the $PaCO_2$; as a surrogate measure, $PetCO_2$ was measured during this study. Given the dynamic gradient between end-tidal and arterial CO_2 concentrations, it is likely that at rest the $PetCO_2$ measure is less than the $PaCO_2$ value; however, with the hypercapnic stimulus, the $PetCO_2$ is expected to be greater than the $PaCO_2$ (Tymko et al., 2016). Participants performed room air breathing for two minutes, the latter minute involving paced-breathing at 7.5 breaths per minute (bpm). This paced breathing was held for the remainder of the protocol, except for the two slower and deeper breaths requested immediately after switching to the Douglas bag containing the CO_2 gas mixture. Participants were instructed to maintain paced breathing for 30 seconds following the two deep breaths, and for two minutes upon returning to breathing room air. Our pilot work suggested that these two deep inspirations leading into the 30-second transient CO_2 paced-breathing allowed for a greater $PetCO_2$ response. This approach was rationalized from the understanding that the two breaths would allow for a rapid equilibration of the gas exchange environment for optimal ventilation to perfusion of the

increased CO_2 (Ainslie & Duffin, 2009; Ito et al., 2008). A recovery period of two minutes followed immediately, while continuing the paced breathing. Ultrasound scanning was maintained throughout the protocol.

Measurements of the $PetCO_2$ and respiratory parameters, notably respiratory rate (RR) and ventilation (VE), were performed using a metabolic cart (Parvo Medics True One system, Sandy, UT, USA). This metabolic cart interfaced with the mouthpiece that the participants breathed through during the entirety of the testing; during the hypercapnic breathing portion of the test, the mouthpiece was connected to the Douglas bag as an intake source. The transient hypercapnic breathing protocol was designed to stimulate shear-mediated vasodilation in the ICA and similar versions of the protocol have been performed successfully in comparable populations (Carr et al., 2020; Hoiland et al., 2017; Smith et al., 2019), however, this thesis study presents a novel methodology for hypercapnia by using the 9% CO_2 Douglas bag for transient breathing, along with the coached deep ventilation (two breaths) prior to initiating the 30-second hypercapnic timer with paced-breathing. The goal was to provide an easy and reproducible method to increase $PaCO_2$ transiently to provoke a vascular stimulus and measure shear-mediated vasodilation in the ICA. The transient hypercapnic period coupled with the paced breathing aimed to avoid hypercapnic-induced hyperventilation following the removal of the brief hypercapnic stimulus. Removal of the CO_2 stimulus following a more prolonged hypercapnia increases cardiorespiratory drive, resulting in confounding hypocapnic vasoconstriction; this would likely counter the expected vasodilatory response provoked by the shear stress.

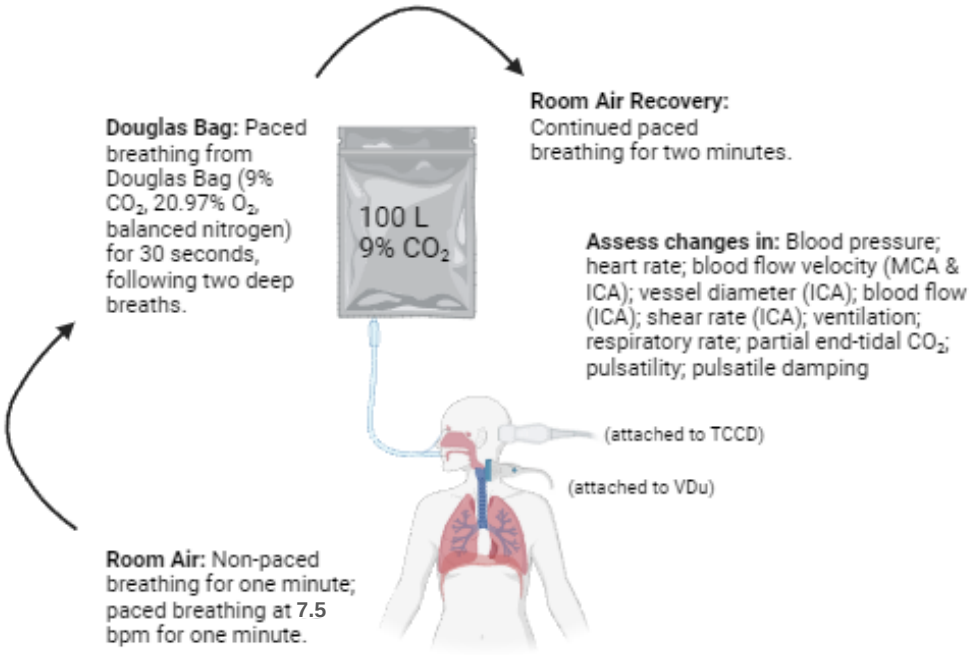

Figure 3.2. Methodological schematic of the breathing test, in which the Douglas Bag is used transiently as the inspiratory line for breathing, to promote hypercapnia and shear-mediated vasodilation in the internal carotid artery (ICA) (Hoiland et al., 2017). The two deep breaths were self-paced, and each participant was asked to breathe slowly and completely (i.e., near full inspiratory capacity). Paced breathing at 7.5 breaths per minute (bpm) is based on a digital metronome count, starting on the second minute of resting baseline measures. TCCD = Transcranial Color-Coded Duplex Ultrasound; VDu = Vascular Duplex Ultrasound. Created with BioRender.com.

3.2.3 Post-Exercise Muscle Ischemia – the Exercise Protocol

Each participant was instructed to breathe at a pace of 7.5 bpm for one minute, followed by three minutes of continuous handgrip exercise using the 30% MVC, whilst continuing the paced breathing. Handgrip exercise was performed using a standardized adjustable handgrip resistance training device (Everlast Adjustable Grip Strengthener, Everlast Canada, ON, CA), whilst verbal coaching was done to mitigate time spent either isometrically contracted or at rest. Resistance was set at 30% MVC (based on the screened value with the dynamometer), thus allowing for dynamic exercise at an initial resistance equal to 30% MVC. Before performing handgrip exercise, participants were fitted to a rapid inflation system via a brachial cuff (Hokanson E20,

Hokanson, WA, USA); this integrated system includes a compressor, compression cuff, and pressure gauge. Functionally, this system allowed for minimal transition time between handgrip exercise and occlusion (~0.3 sec. to full inflation), whilst allowing for precise pressure adjustments.

Following the handgrip exercise period, the exercising limb was occluded; the automatically inflated BP cuff (Hokanson E20, Hokanson, WA, USA) was set to a supra systolic value (i.e., +60 mmHg above peak systolic BP during handgrip) and activated to achieve this occlusion of the upper arm for three minutes, then released for a three-minute recovery period.

3.3 Analysis of Data

The data collected in this study required several considerations when handling, in terms of transforming the ultrasound video files into hemodynamic data, but also in terms of *post hoc* calculations and statistical analysis. In these regards, described below are the procedures and rationales put forth to ensure reliable results for interpretation later in this thesis.

3.3.1 Calculations

Several calculations informed measures of hemodynamic changes in cerebral vasculature during the breathing and PEMI tests. Blood flow in the ICA (Q_{ICA}) (mL/min.) was calculated using the following formula:

$$Q\left(\frac{mL}{minute}\right) = \pi(radius^2)(mean\ envelope\ velocity)\left(\frac{60\ seconds}{minute}\right)$$

The vessel radius was derived from halving the interpreted ICA diameter (ICAd) (cm) using an offline edge-detection software (Woodman et al., 2001), which uses screen-captured video data from the portable VDu; this information was further processed into a data analysis/acquisition

software (LabChart, ADInstruments, CO, USA). Mean envelope velocity was also derived from halving the peak envelope velocity value (cm/s), interpreted from the same edge-detection software.

The shear rate, $\dot{\gamma}$ (/s), was calculated for the ICA, using the following equation:

$$\dot{\gamma}\left(\frac{1}{s}\right) = 4 \times (mean\ velocity)(diameter)$$

This equation relies on Poiseuille's law and makes some assumptions, as follows: (1) The blood is an ideal Newtonian fluid with constant viscosity; (2) the flow is constant and laminar; and (3) the vessel is cylindrical and inelastic (Papaioannou & Stefanadis, 2005).

Based on measured arterial pressure from the photoplethysmography monitoring (hNIBP Nano, ADInstruments, CO, USA), MAP was calculated using the following formula:

$$MAP\ (mmHg) = \left(\frac{1}{3}\right)(systolic\ pressure) + \left(\frac{2}{3}\right)(diastolic\ pressure)$$

All pressure values were interpreted in mmHg. The MAP calculation for the resting BL minute compared to the resting BP measure, where the % difference was used to determine an absolute value (±) applied to the entire participant MAP dataset, specific to each test's BL MAP calculation. A table is provided below, to reflect the MAP adjustment (Table 3.1).

The adjusted MAP value was used in tandem with the MCA flow velocity (MCAv) to calculate CVC and CVR for the intracranial vessel:

$$CVC\ \left(\frac{cm}{s\ \times mmHg}\right) = \frac{MCAv}{MAP}$$

$$CVR\ \left(\frac{mmHg\ \times s}{cm}\right) = \frac{MAP}{MCAv}$$

The PI is related to the peak and trough velocity measures taken at both the MCA and ICA during each test. To calculate the PI (ratio) for both the ICA and MCA, the following equation was used:

$$PI\ (arb.unit\ ratio) = (systolic\ velocity - diastolic\ velocity) \div (mean\ velocity)$$

These calculated PI values further informed the calculation of DFi, using the following equation:

$$DFi\ (arb.unit\ ratio) = (ICA\ PI) \div (MCA\ PI)$$

Although these measures of Q_{ICA}, γ, CVC, CVR, PI, and DFi are descriptive of hemodynamic change, it must be acknowledged that these calculations ultimately rely on the edge-detection software's reliability accuracy with repeated measures, which has been previously validated (Woodman et al., 2001), and is further described in the following subsection (section 3.3.2).

3.3.2 Blood Flow Analysis

Measures of CBF were assessed using the aforementioned offline edge-detection software, which allows for assessing concurrent changes in ICA velocity (ICAv) and ICAd using the VDu, thus the ability to calculate Q_{ICA} accurately (Woodman et al., 2001). For MCA measures from the TCCD, only the flow velocity can be accurately calculated by the edge-detection software; so, although measures of MCA diameter were recorded, they were not assessed for this reason. This software was used with the video files recorded from the portable ultrasound machines and the sampling values were standardized between participants (3 cardiac cycles; "Vivid I" preset for TCCD videos; "Terason T3000" preset for VDu videos). The region of interest (ROI) for edge-detection was set for each individual participant's video files, along with the appropriate scaling factor based on the corresponding ultrasound's scaling settings. The approach of using this edge-detection software is limited by video quality.

Once the edge-detection was run, a comma-separated value (CSV) file was output by the software (Woodman et al., 2001). This file type was read by the software to calculate CBF measures, then further transformed into a file type read by LabChart (text delimited file) (LabChart, ADInstruments, CO, USA) for additional calculations of PI and DFi, as described above (section 3.3.1).

3.3.3 Statistical Analysis

Based on initial power calculations (one-way repeated measures analysis of variance [ANOVA]; partial $\eta^2 = 0.25$, $\alpha = 0.1$, power [1-β] = 0.9, correlation = 0.3) (Hoiland et al., 2017; Jarvis et al., 2011), this study required a minimum of 26 participants (13 biological females) after 20% expected attrition, to achieve sufficient statistical power in terms of relating metaboreflex-dependent BP and HR responses to endothelial function in the ICA. All *post hoc* statistical analysis was done using RStudio (RStudio IDE, PositSoftware, MA, USA) (Appendix B). Using *z*-scores, the extreme statistical outliers were removed from each dataset ($z > 3.29$); in other words, the datasets that are assessed below represent the 99.9% confidence interval (CI) of their original dataset.

One-way repeated measures ANOVA testing was used on the primary outcomes with repeated measures. Given the assumptions for ANOVA testing, additional testing was done to confirm reliability based on these assumptions: homogeneous variance of all measures and normality in the measures' distributions. Homogeneity of variance was assessed using Bartlett's test, in which a *p*-value $\geq \alpha$ (set to 0.05) indicated homogenous variance. The normality in the distributions was confirmed via Shapiro-Wilk normality testing, in which a normally distributed measure had a corresponding *p*-value $\geq \alpha$ (set to 0.05). In terms of effect size, the generalized η^2

was reported instead of partial η^2, given its purported decreased sensitivity to experimental design features, where accounting for variance based on multiple variables is difficult (Lakens, 2013; Olejnik & Algina, 2003). Approximate effect size values for generalized η^2, compared to Cohen's *d*, are suggested as small ($\eta^2 = 0.01$), medium ($\eta^2 = 0.06$), and large ($\eta^2 = 0.14$) effects, though direct comparisons between relevant studies' generalized η^2 is preferable (Cohen, 1988).

All inter-measure comparisons were done using pairwise paired *t*-tests, with a *p*-value adjustment based on the Bonferroni correction (Bonferroni, 1936); this correction factor allowed for more reliable avoidance of false-positive significance (Type I error) in these datasets with multiple complex measures (Armstrong, 2014; Jafari & Ansari-Pour, 2019). As with these specific physiological measures, the significance of comparisons may be resultant of inter-scanner variability or equipment malfunction, thus the correction was used to mitigate inaccurate notions of significance.

For assessing interactions between endothelial function measures during the hypercapnic breathing test and PEMI responses in the handgrip with subsequent occlusion, a Pearson correlation was used. Similar correlation analysis was performed between the change in diameter of the ICA to the area under the curve (AUC) of the ICA $\dot{\gamma}$, from the beginning of the CO_2 stimulus (i.e., Douglas bag breathing) during the hypercapnic breathing test, to the time of peak diameter (s) (Hoiland et al., 2017). Pearson's correlation coefficient (*r*) describes the covariance between the two measures and its interpretation varies, though for this thesis, the following indices were used: negligible correlation ($r = 0$-0.19), weak correlation ($r = 0.2$-0.39), moderate correlation ($r = 0.4$-0.69), strong correlation ($r = 0.7$-0.89), very strong correlation ($r = 0.9$-1) (Overholser & Sowinski, 2008).

In terms of sex-comparative testing, if the dataset indicated large inter-sex group mean differences based on visualization, a Kruskal-Wallis test (Kruskal & Wallis, 1952) was used to inform any sex-dependent variability analysis. This test was also used if multiple measures of the same physiological outcome failed the Shapiro-Wilk testing ($p < 0.05$) within the same protocol. The non-parametric Kruskal-Wallis test provided greater statistical power when assessing group mean variances in the unequal inter-sex sample sizes and when violations of assumptions were inferred, compared to the traditional one-way ANOVA (Nahm, 2016); effect sizes in these tests are represented with the H-statistic equivalent of η^2 (η^2_H). If significance between groups was identified based on the ranked values in the Kruskal-Wallace test, a pairwise comparison was performed using Dunn's test (Dunn, 1964). This test accounts for the rankings of the non-parametric comparisons and familywise error rate when used with the Bonferroni correction (Dinno, 2015). As later discussed, these sex-comparative inferences only serve to illustrate the possible implications of variable sex hormone levels on cardiorespiratory and hemodynamic measures; the comparisons do not give insight into significant absolute differences in physiological responses between males and females.

Chapter 4: Results

4.1 Sample Characteristics

A total of 28 subjects (11 biological females, 17 biological males; 23.6±4.2 years of age; BMI of 24.0±3.2 kg/m^2) were recruited for this study; given an initial attrition of 4% (one female), 27 subjects informed the data for this thesis study. Each of these 27 final participants had successfully completed the entirety of both the transient hypercapnic breathing and handgrip with subsequent PEMI protocols; however, due to technical errors and/or scanner instability, some within-protocol stage measures were unobtainable for certain participants. For these instances, the lost stage of measurement (i.e., minute) was not included for analysis, notably for ICA measures during the transient hypercapnic breathing test (n = 5); thus, the total attrition for the breathing test was 21% (four males, two females) (n = 22). As for the handgrip and subsequent PEMI testing, the same errors resulted in a net 14% attrition (two males, two females) (n = 24). As several cardiorespiratory and hemodynamic measures were assessed, including physiologically relevant data points to the group means was pertinent.

4.2 Characterization of Endothelial Function

The results of the transient hypercapnic breathing test are provided below in detail; the primary measures for characterizing endothelial function during this test are described first, followed by secondary cardiovascular measures for this test that are non-characteristic of endothelial function mechanisms, with the final portion describing the hemodynamic pulsatility and damping from extracranial to intracranial measures.

4.2.1 Cardiorespiratory and Hemodynamic Responses to Transient Hypercapnia

A significant increase in $PetCO_2$ to reflect the transient hypercapnic breathing was observed in the sample population between at least two measures (stages) (F[1.78, 46.23)] = 232.04, p < 0.001, generalized η^2 = 0.71). Using *post hoc* pairwise paired t-testing (α = 0.05), the only significant within-subject differences were found when comparing the baseline testing stages (BL1, BL2) to the Douglas Bag breathing stage (CO2); from BL1 (40.13±6.11 mmHg) and BL2 (39.68±5.62 mmHg), the $PetCO_2$ significantly increased to the CO2 stage (61.06±4.58 mmHg; both p < 0.001). The hypercapnic increase in $PetCO_2$ did not result in significant hypocapnia post-Douglas bag removal (REC1, REC2) when comparing the known resting paced-breathing value in BL2 to the REC1 measure (39.33±5.79 mmHg; p = 1.0) and the REC2 measure (39.33±5.79 mmHg; p = 0.074).

In terms of VE and RR, there was also a significant increase during the hypercapnic breathing protocol (F[2.27, 54.55] = 9.198, p < 0.001, generalized η^2 = 0.12; F[4, 96] = 4.26, p = 0.003, generalized η^2 = 0.11, respectively). That said, it must be noted that the BL2, REC1, and REC2 stages were not normally distributed measures for both VE and RR (all p < 0.05). The comparison between stages illustrates a significant change in VE and RR from the baseline non-paced breathing stage (BL1) to paced breathing measure (BL2); paced breathing in BL2 resulted in a greater VE (11.0±3.74 L/min), but a lower RR (9.60±2.33 bpm) compared to the VE (9.31±2.57 /min; p = 0.026) and RR (11.8±3.30 bpm; p = 0.021) in BL1. However, the change in VE was not significant from BL2 to CO2 (11.9±2.62 L/min.; p = 1.0), to REC1 (12.3±3.31 L/min.; p = 0.95), or to REC2 (9.93±3.07 L/min.; p = 1.0). During recovery, a significant decrease in VE from REC1 to REC2 was observed (p < 0.001), even when breathing remained consistent (9.31±2.46 to 9.61±2.07 bpm; p = 1.0).

The ICA $\dot{\gamma}$ values during the breathing test showed similar trends to $PetCO_2$ measures; a significant change was observed throughout the breathing test (F[2.36, 44.83] = 33.725, p < 0.001, generalized η^2 = 0.24), as expected to probe shear-mediated mechanisms. Significance was found when comparing BL1 (322.10±105.94 /s) and BL2 (316.55±101.93 /s) stages to the CO2 stage (409.73±155.35 /s; both p < 0.001), but no significant change from BL1 to BL2 was observed (p = 1.0). Additionally, no significant change was observed between REC1 (312.72±109.69 /s) and REC2 (269.71±95.53 /s; p = 0.14), but significant decreases in RR occurred when comparing BL2 to REC2 (p = 0.004), which is not consistent with the $PetCO_2$ measures.

Stages	$PetCO_2$ (mmHg)		VE (L/min.)		RR (bpm)		ICA $\dot{\gamma}$ (/s)	
	Mean	SD (±)	Mean	SD (±)	Mean	SD (±)	Mean	SD (±)
BL1	40.13	6.11	9.31	2.57	11.8	3.30	322.10	105.94
BL2	39.68	5.62	11.0	3.74	9.60	2.33	316.55	101.93
CO2	61.06**	4.58	11.9	2.62	10.1	2.95	409.73**	155.35
REC1	39.33	5.79	12.3	3.31	9.31	2.46	312.72	109.69
REC2	38.15	5.98	9.93	3.07	9.61	2.07	269.71*	93.53

Table 4.1. Table detailing the group mean values and corresponding standard deviations (SD) for the partial pressure of end-tidal CO_2 ($PetCO_2$), ventilation (VE), respiratory rate (RR), and shear rate ($\dot{\gamma}$) in the internal carotid artery (ICA) during each stage of the transient hypercapnic breathing protocol. *Indication of significance in pairwise paired t-test (p < 0.05), relative to the paced-breathing baseline (BL2) measures; **denotes significance of p < 0.001. ‡Indication of significance (p < 0.05) in comparisons proceeding the hypercapnic Douglas bag breathing stage (CO2), relevant for measures of shear-mediated vasodilation.

Figure 4.1 illustrates the trends in $PetCO_2$, VE, RR, and ICA $\dot{\gamma}$ measures. The results for ICA $\dot{\gamma}$ appear to be differentially variant between males and females, following sex-comparative analysis (p = 0.013). Additionally, a moderate effect was observed when comparing the group means of males and females in terms of ICA $\dot{\gamma}$ (η^2_H = 0.122). Inter-measure pairwise comparisons show significance only for the decrease in ICA $\dot{\gamma}$ observed in males, following the

CO2 stage: after CO2 (336±98.18 /s), ICA $\dot{\gamma}$ in REC1 decreased to 251.34±55.89 /s (p = 0.037) and to 229.17±67.08 /s in REC2 (p = 0.0025).

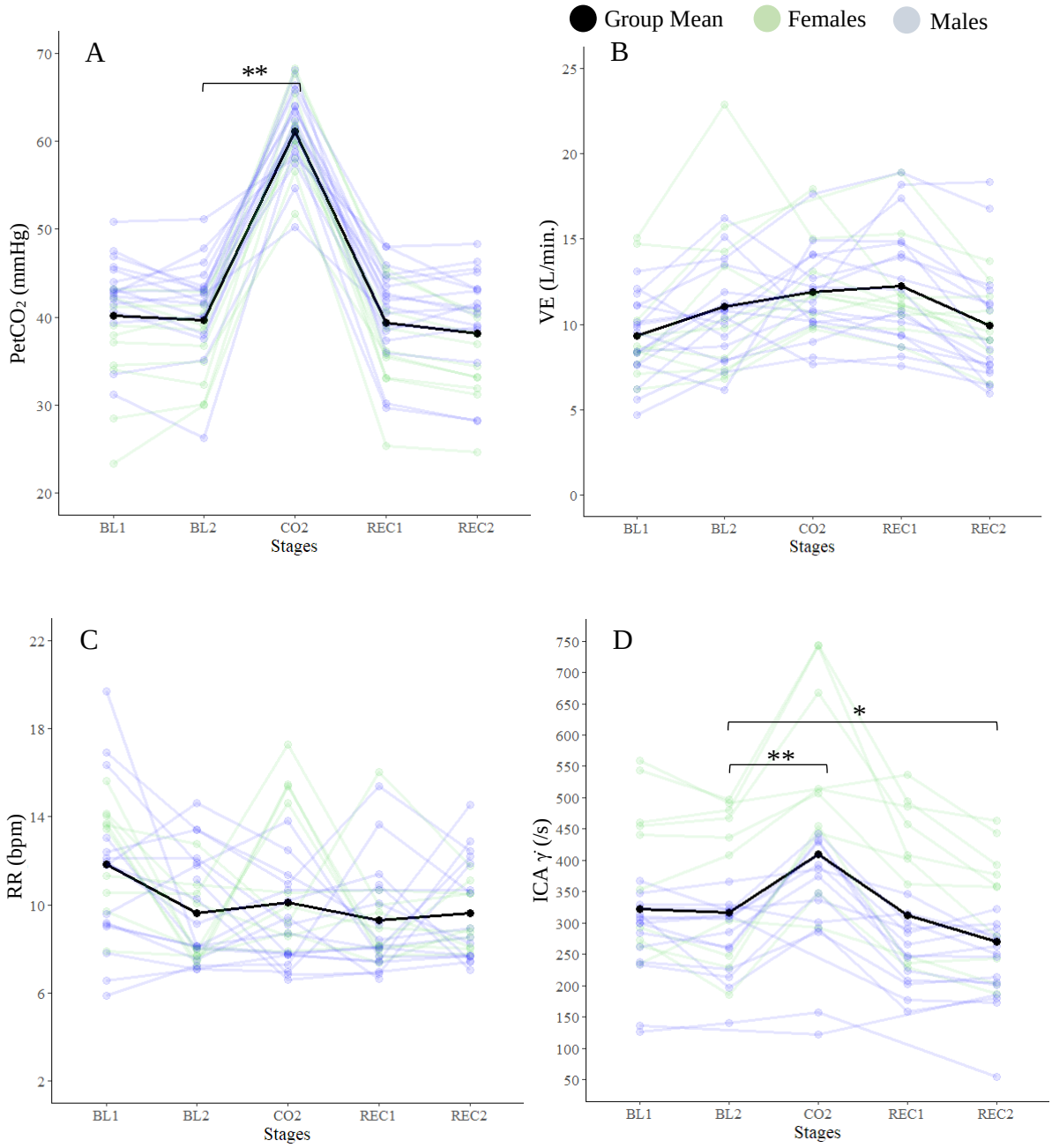

Figure 4.1. Scatterplot graphs for the (A) partial pressure of end-tidal CO_2 ($PetCO_2$), (B) ventilation (VE), (C) respiratory rate (RR), and (D) shear rate ($\dot{\gamma}$) in the internal carotid artery (ICA), during the transient hypercapnic breathing protocol. Group means are represented by the black line, females' values are green, and males' values are blue. *Indication of significance in pairwise paired t-test ($p < 0.05$), relative to the paced-breathing baseline (BL2) measures; **denotes significance of $p < 0.001$. ‡Indication of significance ($p < 0.05$) in comparisons proceeding the hypercapnic Douglas bag breathing stage (CO2), relevant for measures of shear-mediated vasodilation.

Given that the absolute change in ICA $\dot{\gamma}$ does not inform sex-comparative measures based on these results, the relevant change scores are illustrated below for males and females (Figure 4.2) to better visualize inter-sex variance that was not accounted for. The comparisons are based on the significant stage comparisons observed in the total sample data (Table 4.1) and inter-sex pairwise testing: for the change in ICA $\dot{\gamma}$ from BL2 to CO2, females had a median +49.9%$\Delta\dot{\gamma}$ (IQR = 53.6) and males had a median +31.1%$\Delta\dot{\gamma}$ (IQR = 35.1); from CO2 to REC1, females had a median -32.6%$\Delta\dot{\gamma}$ (IQR = 12.8) and males had a median -32.1%$\Delta\dot{\gamma}$ (IQR = 15.4); finally, from CO2 to REC2, females had a median -46.3%$\Delta\dot{\gamma}$ (IQR = 15.6) and males had a median -31.8%$\Delta\dot{\gamma}$ (IQR = 17.8).

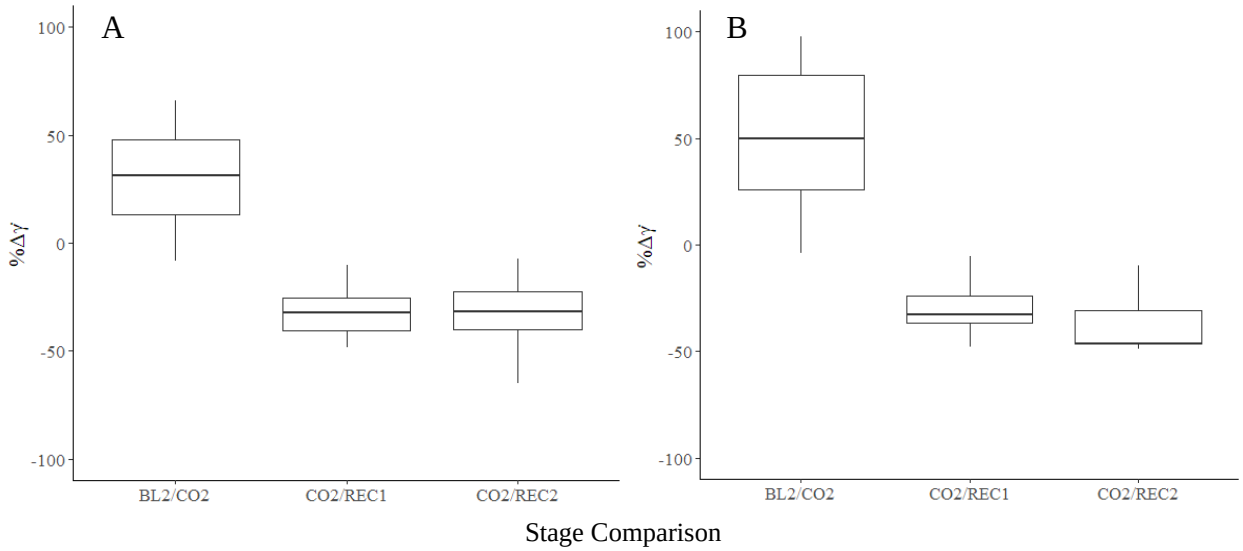

Figure 4.2. Boxplot graphs for the (A) female and (B) male shear rate ($\dot{\gamma}$) percent changes in the internal carotid artery (ICA); the first stage comparison from the left on each panel is between the paced breathing baseline stage (BL2) to the Douglas bag breathing stage (CO2) (BL2/CO2), followed by the CO2 stage compared to the first minute of atmospheric air breathing post-hypercapnia (REC1) (CO2/REC1), and the CO2 stage compared to the second minute of atmospheric air breathing post-hypercapnia (REC2) (CO2/REC2).

For measures of ICAd, a significant change in average vessel diameter was observed during the protocol (F[4, 80] = 3.013, p = 0.023, generalized η^2 = 0.012). To ensure that there is sufficient sensitivity for diameter change analysis, thus avoiding type II error, there was no Bonferroni correction applied to pairwise testing (Armstrong, 2014; Jafari & Ansari-Pour, 2019);

results of these comparisons show a significant increase in ICAd from BL1 (0.496±0.05 cm) to REC1 (0.515±0.07 cm; $p = 0.044$) and REC2 (0.510±0.07 cm; $p = 0.036$), as well as significant increases from BL2 (0.495±0.06 cm) to REC2 ($p = 0.034$) (Table 4.2). Most pertinently, there was a significant increase in ICA diameter from CO2 (0.492±0.08 cm) to REC1 ($p = 0.021$), suggestive of vasodilation as described by the relationship between ICA $\dot{\gamma}$ and vessel diameter from the start of hypercapnic breathing (CO2 stage).

Stages	ICAd (cm)		ICAv (cm/s)		Q_{ICA} (mL/min.)	
	Mean	SD (±)	Mean	SD (±)	Mean	SD (±)
BL1	0.496	0.05	39.94	12.15	242.21	88.13
BL2	0.495	0.06	38.88	11.13	234.51	84.84
CO2	0.492	0.08	48.22**	13.81	305.88**	106.69
REC1	0.515‡	0.07	39.20	11.53	245.63	83.49
REC2	0.510*	0.07	33.97*	10.21	210.57	67.08

Table 4.2. Table detailing the group mean values and corresponding standard deviations (SD) for the internal carotid artery diameter (ICAd), ICA blood flow velocity (ICAv), and ICA volumetric flow (Q_{ICA}). *Indication of significance in pairwise paired t-test ($p < 0.05$), relative to the paced-breathing baseline (BL2) measures; **denotes significance of $p < 0.001$. ‡Indication of significance ($p < 0.05$) in comparisons proceeding the hypercapnic Douglas bag breathing stage (CO2), relevant for measures of shear-mediated vasodilation.

Figure 4.3 illustrates the change in ICAd throughout the hypercapnic breathing protocol (panel A), as well as the time to peak diameter after the start of the CO2 stage (panel B). Time to peak information is supportive of significant diameter changes from CO2 to REC1, given the total group median (46.2 s; IQR = 13.4) and mean (47.0±11.2 s) being within the minute proceeding the change from Douglas bag breathing back to room air (REC1 stage). Sex-comparative visualization of time to peak ICA diameter does not suggest a large absolute difference between males (46.2 s; IQR = 9.57) and females (46.4 s; IQR = 22.9), but further corroborates the possible sex-dependent variability in ICA $\dot{\gamma}$ given larger variability in females.

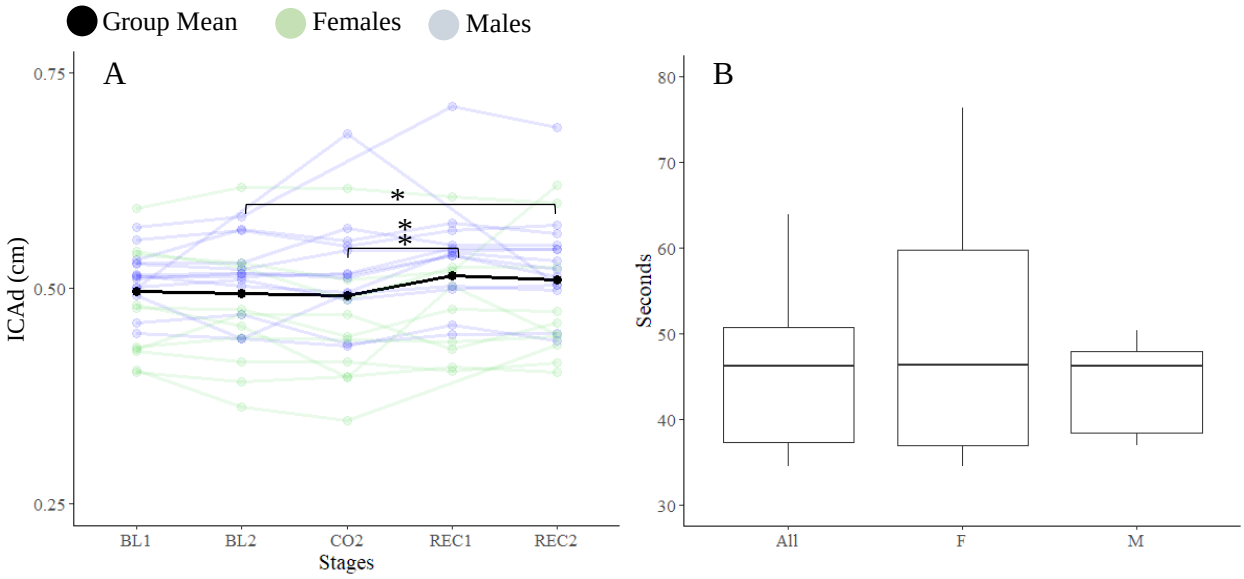

Figure 4.3. Scatterplot (A) and boxplot (B) graphs related to changes in internal carotid artery diameter (ICAd) during the transient hypercapnic breathing test: (A) the left panel shows group changes in ICAd per stage, where group means are represented by the black line, females' values are green, and males' values are blue; (B) the right panel shows time to peak diameter starting from the initial inspiration from the Douglas bag, with mean total group data (ALL), female data (F), and male data (M) displayed. *Indication of significance in pairwise paired t-test ($p < 0.05$), relative to the paced-breathing baseline (BL2) measures; ‡denotes significance of $p < 0.05$ in comparisons relative to the hypercapnic Douglas bag breathing stage (CO2), relevant for measures of shear-mediated vasodilation.

To further visualize ICAd responses to shear stress as a measure of endothelial function during this test was to correlate the peak percent change (%Δ) in ICAd with the ICA γ̇ AUC; the results of this comparison are visualized below (Figure 4.4, panel A) and show a weak and non-significant positive correlation between the %ΔICAd and ICA γ̇ AUC ($r = 0.23$, $p = 0.3$). When the correlation is adjusted to show only participant values within the 95% CI from the original correlation, the relationship strengthens to significance ($r = 0.86$, $p < 0.001$). Peak %ΔICAd before adjusting for extraneous values was 9.56±9.33%, while post-adjustment results in a peak ΔICAd of 6.77±3.97%.

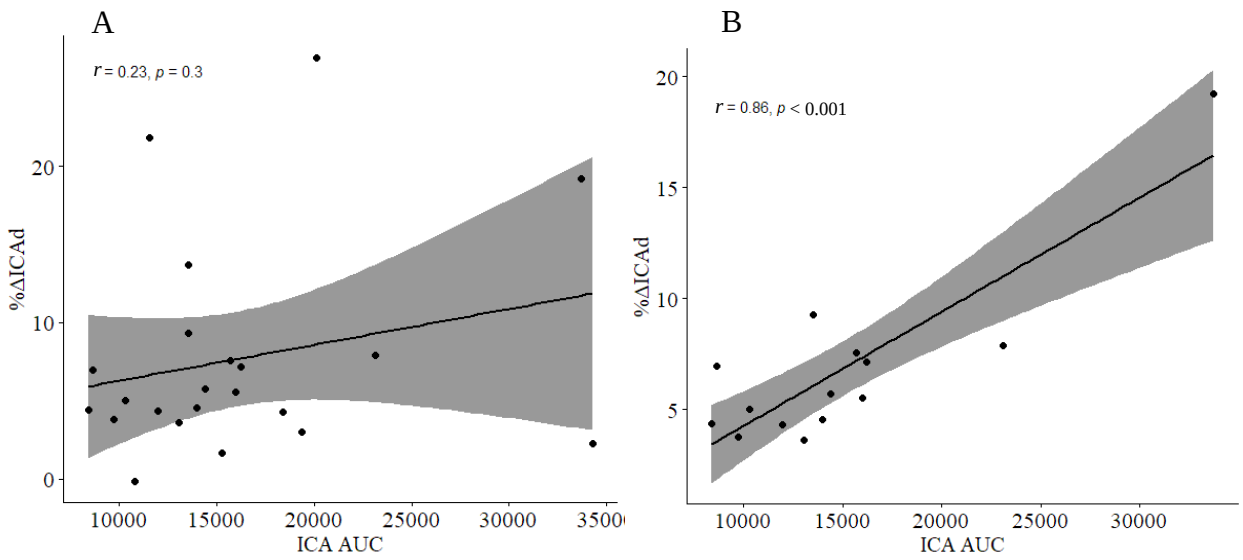

Figure 4.4. Scatterplot graph (A) plotting the correlation between the internal carotid artery (ICA) shear rate $\dot{\gamma}$ area under the curve (AUC), calculated from the start of the Douglas bag breathing stage (CO2) at 120 seconds (two minutes) into the protocol to the time when the peak diameter occurs per individual, against the peak change in ICA diameter (%ΔICAd), for each participant (n = 22). The right panel (B) shows the adjusted correlation with the values extraneous to the 95% confidence interval (CI) of the plot on the left panel (A) removed (n = 14).

Extracranial velocity measures follow similar trends to those observed with ICA $\dot{\gamma}$; there was a significant change in ICAv during the hypercapnic breathing test (F[4, 72] = 39.075, $p < 0.001$, generalized $\eta^2 = 0.299$) and significance was found for the comparison between BL1 (39.94±12.25 cm/s) and REC2 (33.97±10.21 cm/s; $p = 0.004$), as well as BL2 (38.88±11.13 cm/s) to REC2 ($p = 0.008$). Pertinently, significant differences in ICAv measures were observed from both BL1 and BL2 measures to the CO2 stage (48.22±12.25 cm/s; both $p < 0.001$) and from CO2 to REC1 (39.20±11.53 cm/s) and REC2 (both $p < 0.001$). There was also a significant difference in Q_{ICA} during the hypercapnic breathing test (F[4, 80] = 28.135, $p < 0.001$, generalized $\eta^2 = 0.156$). Similar to ICAv measures, significant differences in Q_{ICA} were observed from both BL1 (242.21±88.13 mL/min.) to CO2 (305.88±106.69 mL/min.; $p < 0.001$) and from BL2 (234.51±84.84 mL/min.) to CO2 ($p < 0.001$). Comparison between CO2 and the recovery stages showed a significant increase to REC1 (245.63±83.49 mL/min.) and REC2 (210.57±67.08 mL/min.; both $p < 0.001$). Also trending with ICAv measures, there was a significant decrease

between BL1 and REC2 ($p = 0.044$), but inconsistent with ICAv results, there was no significant difference observed from BL2 to REC2 ($p = 0.18$). Visualizations in the measures of ICAv and Q_{ICA} are also provided below (Figure 4.3).

The ICAv distribution appears to be different between males and females; sex-comparative analysis shows significance during the test ($p = 0.02$, $\eta^2_H = 0.096$). Inter-measure pairwise comparisons show significance only for the decrease in ICAv observed in males, following the CO2 stage: after CO2 (43.64±8.92 cm/s), ICAv in REC1 decreased to 33.57±6.89 cm/s ($p = 0.014$) and to 30.42±7.99 cm/s in REC2 ($p < 0.001$), which was consistent with the comparisons of ICA $\dot{\gamma}$. The relevant change scores for ICAv are illustrated below for males and females (Figure 4.5) to better visualize inter-sex variance that was not accounted for. For the change in ICAv from BL2 to CO2, females had a median +44.7%ΔICAv (IQR = 57.4) and males had a median +31.5%ΔICAv (IQR = 17.7); from BL2 to REC2, females had a median -10.9%ΔICAv (IQR = 22.0) and males had a median -10.6%ΔICAv (IQR = 19.9); from CO2 to REC1, females had a median -30.1%ΔICAv (IQR = 10.3) and males had a median -28.9%ΔICAv (IQR = 14.2); finally, from CO2 to REC2, females had a median -36.5%ΔICAv (IQR = 18.7) and males had a median -28.2%ΔICAv (IQR = 18.9).

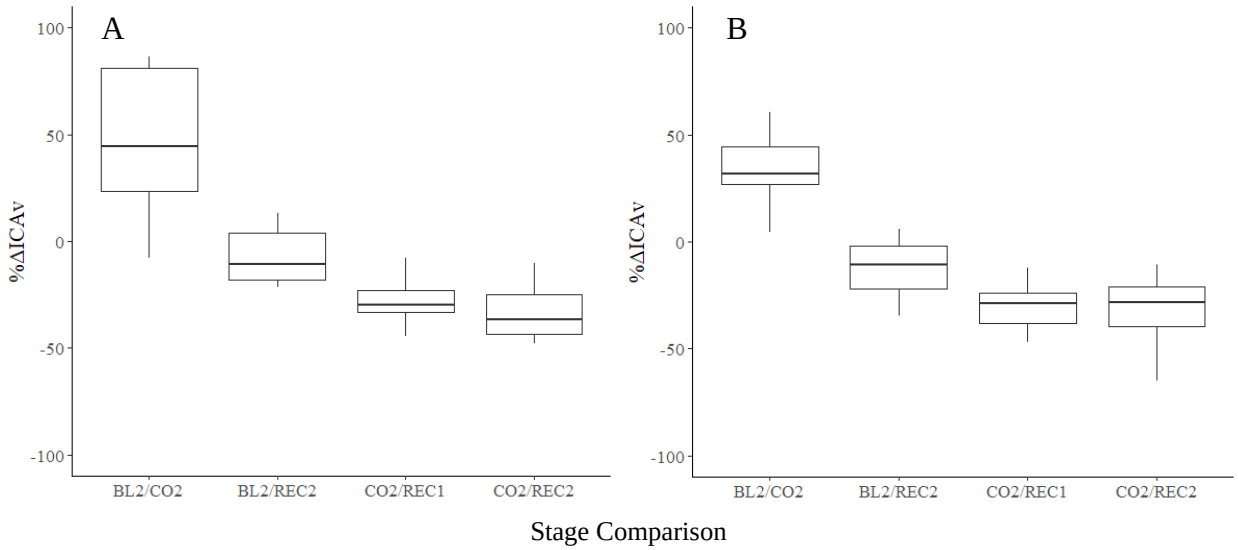

Figure 4.5. Boxplot graphs for the (A) female and (B) male internal carotid artery velocity (ICAv) percent changes; the first stage comparison from the left on each panel is between the paced breathing baseline stage (BL2) to the Douglas bag breathing stage (CO2) (BL2/CO2), followed by the BL2 stage compared to the second minute of atmospheric air breathing post-hypercapnia (REC2), the CO2 stage compared to the first minute of atmospheric air breathing post-hypercapnia (REC1) (CO2/REC1), and the CO2 stage compared to the REC2 stage (CO2/REC2).

4.2.2 Secondary Cardiovascular and MCAv Outcomes

In terms of MAP results, values were adjusted based on the resting BL reading with the automatic cuff; the % difference between the BL hNIBP and automatic cuff measures was used to adjust all values of MAP, per participant and per test, to achieve more physiologically relevant BP monitoring (Appendix A). The results for MAP during this test indicated a significant difference between at least two stage measures (F[2.98, 74.51] = 3.849, p = 0.013, generalized η^2 = 0.045). Though, the only significant stage comparison based on pairwise testing was from BL2 (83.47±8.40 mmHg) to CO2 (88.58±7.59 mmHg). As for HR, REC1 and REC2 stage measures were non-normally distributed, thus proceeding non-parametric analysis did not suggest a significant difference between any stage measures (p = 0.296). The table below (Table 4.3) describes these MAP and HR values throughout the hypercapnic breathing test. Note that units

for HR are beats per minute (bpm); though this abbreviation conflicts with the described units for RR, these are distinct measures.

Stages	MAP (mmHg)		HR (bpm)		MCAv (cm/s)	
	Mean	SD (±)	Mean	SD (±)	Mean	SD (±)
BL1	85.79	5.74	66.46	8.54	66.62	18.29
BL2	83.47	8.40	70.55	9.59	61.71	15.04
CO2	88.58*	7.59	69.04	9.00	84.45**	16.90
REC1	85.35	8.31	67.75	10.02	63.00	14.33
REC2	86.36	5.26	66.36	8.17	56.58	12.26

Table 4.3. Table detailing the group mean values and corresponding standard deviations (SD) for the mean arterial pressure (MAP), heart rate (HR), and the middle cerebral artery blood flow velocity (MCAv) during the transient hypercapnic breathing test. *Indication of significance in pairwise paired t-test ($p < 0.05$), relative to the paced-breathing baseline (BL2) measures; **denotes significance of $p < 0.001$. ‡Indication of significance ($p < 0.05$) in comparisons proceeding the hypercapnic Douglas bag breathing stage (CO2), relevant for measures of shear-mediated vasodilation.

The MCAv results indicate that there were significant differences between at least two stage measures ($F[2.55, 58.7] = 37.676$, $p < 0.001$, generalized $\eta^2 = 0.364$). As with the HR measures, multiple stages measures for MCAv violated the test for normality: BL2 ($p = 0.023$), REC1 ($p = 0.004$), and REC2 ($p = 0.024$). Non-parametric analysis still suggested a significant difference between at least two measures ($p < 0.001$; $\eta^2_H = 0.210$); significance was found for the comparison between BL1 (66.62±18.29 cm/s) and CO2 (84.45±16.90 cm/s; $p = 0.01$), as well as BL2 (61.71±15.04 cm/s) to CO2 ($p < 0.001$). Additionally, significant differences in MCAv measures were observed from CO2 to REC1 (63.00±14.33 cm/s; $p = 0.002$) and REC2 (56.58±12.26 cm/s; $p < 0.001$). Measures of ICAv and MCAv only trended differently when comparing BL1 to REC2, as this was a non-significant finding for MCAv measures ($p = 0.3$).

Most stage measures of CVR in the MCA were not distributed normally, thus non-parametric analysis suggested that there were several significant stage comparisons ($p < 0.001$, $\eta^2_H = 0.168$);

corresponding CVR measures were distributed normally and significance between at least two stage measures was indicated ($F[4, 88] = 28.022$, $p < 0.001$, generalized $\eta^2 = 0.277$). Significant increases in CVC were observed from BL1 (0.78±0.23 cm/[mmHg•s]) and BL2 (0.75±0.21 cm/[mmHg•s]) to CO2 (0.95±0.18 cm/[mmHg•s]; $p = 0.034$ and $p = 0.004$, respectively). The same results were observed for CVR, though inversely, as there was a significant decrease BL1 (1.38±0.37 ([mmHg•s]/cm) and BL2 (1.42±0.32 ([mmHg•s]/cm) to CO2 (1.10±0.24 ([mmHg•s]/cm; both $p < 0.001$). For CVC, there was also a significant decrease from CO2 to both REC1 (0.74±0.18 cm/[mmHg•s]; $p < 0.001$) and REC2 (0.66±0.15 cm/[mmHg•s]; $p < 0.001$), which was mirrored by an increase in CVR from CO2 to both REC1 (1.42±0.32 [mmHg•s]/cm; $p < 0.001$) and REC2 (1.59±0.33 [mmHg•s]/cm; $p < 0.001$). Unique significant changes in CVR occurred from BL1 to REC2 ($p < 0.001$) and BL2 to REC2 ($p = 0.014$); these comparisons were non-significant for CVC ($p = 0.3$ and $p = 1.0$, respectively). Measures for CVC and CVR during the hypercapnic breathing test are tabulated below (Table 4.4).

Stages	CVC (cm/[mmHg•s])		CVR ([mmHg•s]/cm)	
	Mean	SD (±)	Mean	SD (±)
BL1	0.78	0.23	1.38	0.37
BL2	0.75	0.21	1.42	0.32
CO2	0.95*	0.18	1.10**	0.24
REC1	0.74‡	0.18	1.42‡	0.32
REC2	0.66‡	0.15	1.59‡*	0.33

Table 4.4. Table detailing the group mean values and corresponding standard deviations (SD) for the intracranial cerebrovascular conductance (CVC) and cerebrovascular resistance (CVR) during the transient hypercapnic breathing test. *Indication of significance in pairwise paired t-test ($p < 0.05$), relative to the paced-breathing baseline (BL2) measures; **denotes significance of $p < 0.001$. ‡Indication of significance ($p < 0.05$) in comparisons proceeding the hypercapnic Douglas bag breathing stage (CO2), relevant for measures of shear-mediated vasodilation.

4.2.3 Pulsatility and Damping During with Shear-Mediated Vasodilation

The PI responses for both the MCA and ICA inform the DFi during the hypercapnic breathing test. For ICA PI, there was a significant change indicated between at least two measures (F[4, 80] = 9.235, $p < 0.001$, generalized $\eta^2 = 0.128$). Pairwise testing indicated significant changes between BL1 (1.35±0.43) and REC2 (1.61±0.47; $p = 0.014$), as well as between BL2 (1.42±0.32) and CO2 (1.18±0.31) where ICA PI decreased. Significant differences were also observed between CO2 and both REC1 (1.54±0.44; $p = 0.003$) and REC2 (1.61±0.47; $p = 0.004$). The MCA PI measures resulted in similar significant change between at least two measures, but with a larger effect than observed with ICA PI (F[4, 96] = 21.057, $p < 0.001$, generalized $\eta^2 = 0.258$). In conjunction, the pairwise testing suggested that the MCA PI difference was significant between BL1 (0.87±0.20) and CO2 (0.68±0.09; $p < 0.001$), as well as for BL2 (0.94±0.18) to CO2 ($p < 0.001$). Significant comparisons continued between CO2 and both REC1 (0.92±0.18; $p < 0.001$) and REC2 (0.96±0.18; $p < 0.001$). The similar trends in ICA PI and MCA PI corroborate the notion that no significant differences were observed between stage measures in

terms of DFi during the hypercapnic breathing test (F[4, 76] = 0.835, p = 0.507, generalized η^2 = 0.014), suggesting a maintenance of pulsatile damping throughout the test. Table 4.5 below group averages and standard deviations values for these measures.

Stages	ICA PI (ratio)		MCA PI (ratio)		DFi (ratio)	
	Mean	SD (±)	Mean	SD (±)	Mean	SD (±)
BL1	1.35	0.43	0.87	0.20	1.57	0.38
BL2	1.42	0.32	0.94	0.18	1.52	0.41
CO2	1.18*	0.31	0.68**	0.09	1.77	0.52
REC1	1.54‡	0.44	0.92‡	0.18	1.70	0.48
REC2	1.61‡	0.47	0.96‡	0.18	1.63	0.48

Table 4.5. Table detailing the group mean values and corresponding standard deviations (SD) for the internal carotid artery pulsatility (ICA PI), middle cerebral artery pulsatility (MCA PI), and the damping factor index (DFi) during the transient hypercapnic breathing test. *Indication of significance in pairwise paired t-test ($p < 0.05$), relative to the paced-breathing baseline (BL2) measures; **denotes significance of $p < 0.001$. ‡Indication of significance ($p < 0.05$) in comparisons proceeding the hypercapnic Douglas bag breathing stage (CO2), relevant for measures of shear-mediated vasodilation.

The visualization of DFi (Figure 4.6) depicts the trend of non-significant group mean change over the duration of the test (panel A) and the change values (panel B) further suggest that the stimulus-response does alter the %ΔDFi, but non-significantly during the hypercapnic breathing protocol. The median change rose from -2.09%Δ (IQR = 19.9) to +7.42%Δ (IQR = 24.4) when observing the BL1/BL2 comparison and BL2/CO2 comparison, respectively. The %Δ in DFi trended downwards (-3.92%Δ; IQR = 32.4) into the CO2/REC1 comparison and continued downwards to the REC1/REC2 comparison (-11.4%Δ; IQR = 23.1).

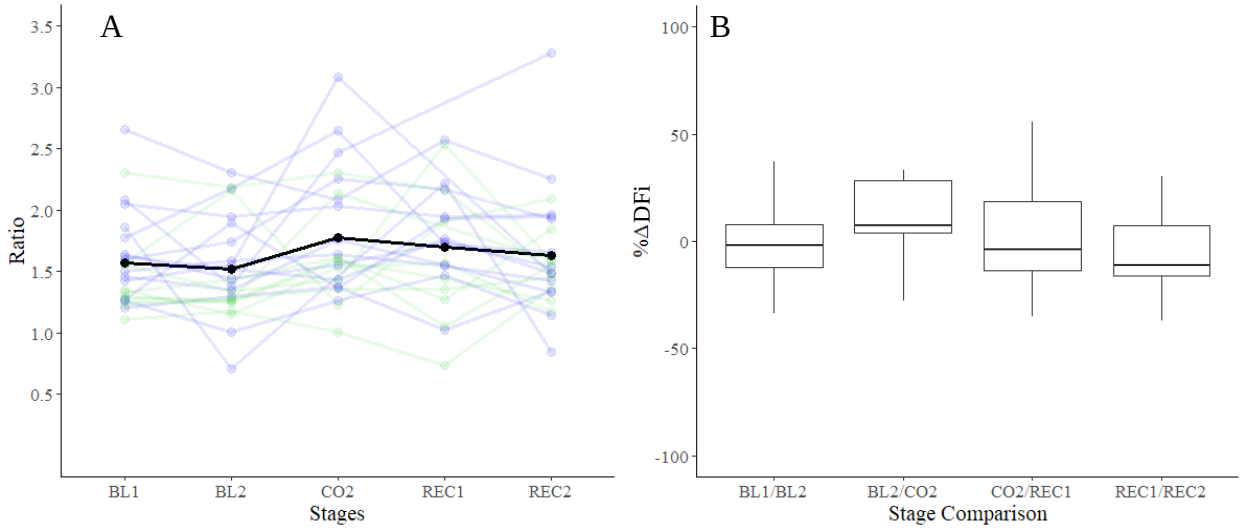

Figure 4.6. Scatterplot (A) and boxplot (B) graphs related to changes in damping factor index (DFi) during the transient hypercapnic breathing test: (A) the left panel shows group changes in DFi per stage, where group means are represented by the black line, females' values are green, and males' values are blue; (B) the right panel shows percent change (%Δ) in DFi per stage comparison. The first stage comparison from the left is between the non-paced breathing baseline stage (BL1) and the paced breathing baseline stage (BL2) (BL1/BL2); the next comparison is of BL2 to the Douglas bag breathing stage (CO2) (BL2/CO2), followed by the CO2 stage compared to the first minute of atmospheric air breathing post-hypercapnia (REC1) (CO2/REC1), and the REC1 stage compared to the second minute of atmospheric air breathing post-hypercapnia (REC2) (REC1/REC2).

4.3 Characterization of Metaboreflex Stimulation

The detailed results of the handgrip exercise and subsequent PEMI testing are provided below; the cardiovascular and cardiorespiratory measures for characterizing metaboreflex responses are provided first, followed by the cerebral hemodynamic measures during this test, then ending the section with the specific pulsatility and damping results related to metaboreflex stimulation.

4.3.1 Cardiovascular and Cardiorespiratory Responses to Handgrip and PEMI

The BP stimuli of handgrip exercise and resulting PEMI are confirmed from the results of this testing; there were significant differences between at least two stage measures (F[2.96, 74] = 15.744, $p < 0.001$, generalized $\eta^2 = 0.214$). Significant differences between stages were observed

from the BL stage (86.31±5.70 mmHg) to all handgrip exercise stages: the first minute of handgrip (HG1) increased MAP to 91.31±6.74 mmHg ($p < 0.001$), the second minute (HG2) to 93.54±8.28 mmHg ($p < 0.001$), and the third minute (HG3) to 96.76±9.60 mmHg ($p < 0.001$). The average peak increase in MAP from BL to handgrip was +12.18±9.24 mmHg. Similarly, there was a significant increase from BL to the PEMI stages: the first minute of occlusion (PEMI1) saw a significant increase to 95.47±11.33 mmHg ($p = 0.002$), as did the second minute (PEMI2) to 96.45±12.71 mmHg ($p = 0.005$); however, the third minute of occlusion (PEMI3) (94.04±14.58 mmHg) did not incur a significant increase from BL ($p = 0.317$). During handgrip, there was a significant increase in MAP, comparing HG1 to HG3 ($p = 0.008$); although there was no significant difference observed between HG1 and all of the post-occlusion recovery stages (REC1, REC2, and REC3) (87.89±6.64 mmHg, 85.09±10.74 mmHg, and 84.20±10.37 mmHg, respectively; all $p > 0.05$). For HG2 compared to REC1, REC2, and REC3, significant differences were observed ($p = 0.013$, $p = 0.006$, and $p = 0.002$, respectively); the same can be said for HG3 compared to REC1, REC2, and REC3 (all $p < 0.001$). MAP appeared to return to BL values when comparing the PEMI stages to all of the recovery stages (all $p \leq 0.02$); uniquely though, PEMI3 did not decrease significantly to REC1 ($p = 0.078$), but was significantly different compared to REC2 and REC3 ($p = 0.035$ and $p = 0.012$, respectively).

In terms of HR, which in tandem with MAP gives more context to cardiovascular responses to metaboreflex stimulation, there were significant differences between at least two stage measures ($F[4.58, 114.43] = 25.838$, $p < 0.001$, generalized $\eta^2 = 0.167$). Pairwise analysis indicated significance for BL (65.46±8.01 bpm) to HG1, HG2, and HG3 (72.61±10.00 bpm, 73.75±11.45 bpm, and 74.11±10.18 bpm, respectively; all $p < 0.001$). Significant differences were not preserved when comparing BL to PEMI1, PEMI2, and PEMI3 (65.71±11.78 bpm, 66.01±10.99

bpm, and 66.33±9.17 bpm, respectively; all $p > 0.05$). Also inconsistent with the results for MAP, there was no significant increase in HR observed when comparing HG1 to HG3 ($p = 1.0$); furthermore, there were significant differences observed between HG1 and all of the post-occlusion recovery stages (REC1, REC2, and REC3) (87.89±6.64 mmHg, 85.09±10.74 mmHg, and 84.20±10.37 mmHg, respectively; all $p < 0.001$). The HG2 and HG3 stages also saw significant decreases to REC1, REC2, and REC3 (all $p < 0.001$). Pertinently for inferences about the impact of the metaboreflex on HR, significant decreases were observed from all three handgrip stages to all three PEMI stages (all $p \leq 0.002$). All values for MAP and HR measures during this test are tabulated below (Table 4.6), as well as visualized (Figure 4.7).

Stages	MAP (mmHg)		HR (bpm)		$PetCO_2$ (mmHg)	
	Mean	SD (±)	Mean	SD (±)	Mean	SD (±)
BL	86.31	5.70	65.46	8.01	39.39	5.10
HG1	91.31**	6.74	72.61**	10.00	37.85	5.85
HG2	93.54**	8.28	73.75**	11.45	36.53*	6.15
HG3	96.76**	9.60	74.11**	10.18	34.94**	6.75
PEMI1	95.47*	11.33	65.71	11.78	35.15*	6.79
PEMI2	96.45*	12.71	66.01	10.99	34.39*	7.32
PEMI3	94.04	14.58	66.33	9.17	33.93**	7.00
REC1	87.89‡	6.64	62.76	7.65	35.96	7.73
REC2	85.09‡	10.74	62.26	9.14	36.05	7.80
REC3	84.20‡	10.37	64.15	7.16	35.97	8.09

Table 4.6. Table detailing the group mean values and corresponding standard deviations (SD) for the mean arterial pressure (MAP), heart rate (HR), and the partial pressure of end-tidal (CO_2) during the handgrip exercise and subsequent post-exercise muscle ischemia (PEMI) testing. *Indication of significance in pairwise paired t-test ($p < 0.05$), relative to the initial baseline (BL) measures; **denotes significance of $p < 0.001$. ‡Indication of significance ($p < 0.05$) in comparisons proceeding the second minute of PEMI (PEMI2), relevant for validating measures of metaboreflex stimulation.

Table 4.5 displays the measures for $PetCO_2$ during the handgrip exercise with subsequent PEMI testing. The results indicate that there were significant differences between stage measures

(F[3.11, 77.78] = 12.082, p < 0.001, generalized η^2 = 0.049), suggesting that $PetCO_2$ was significantly variable during this test despite methodological mitigation. Significant comparisons were observed between the BL (39.39±5.10 mmHg) stage and HG2 (36.53±6.15 mmHg; p = 0.004), HG3 (34.94±6.75 mmHg; p < 0.001), PEMI1 (35.15±6.79 mmHg; p = 0.002), PEMI2 (34.39±7.31 mmHg; p = 0.002), and PEMI3 (33.93±7.00 mmHg; p < 0.001). There was also a significant difference between HG1 (37.85±5.85 mmHg) and HG2 (p = 0.048), HG3 (p = 0.001), PEMI1 (p = 0.021), PEMI2 (p = 0.01), as well as PEMI3 (p < 0.001). Between HG2 and PEMI3 there was a significant decrease in $PetCO_2$ (p = 0.006), then comparing PEMI2 to REC1 and PEMI3 to REC1 there were also significant increases (p = 0.012 and p < 0.001, respectively).

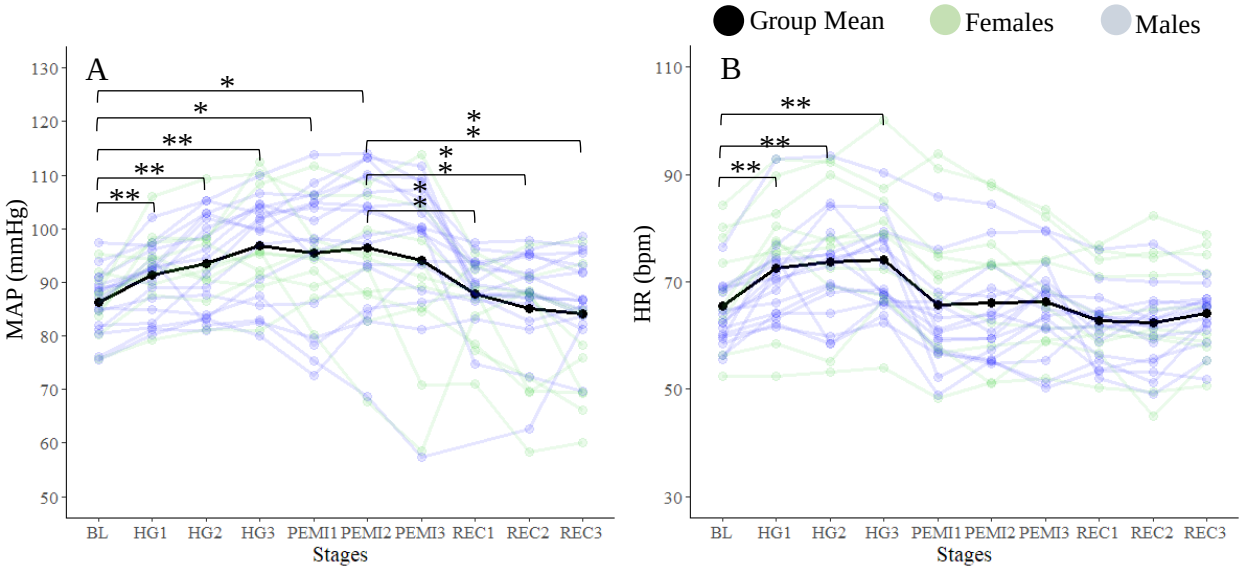

Figure 4.7. Scatterplots illustrating changes in the (A) mean arterial pressure (MAP) and (B) heart rate (HR) during the handgrip exercise and subsequent post-exercise muscle ischemia (PEMI) testing. Group means are represented by the black line, females' values are green, and males' values are blue. *Indication of significance in pairwise paired t-test (p < 0.05), relative to the initial baseline (BL) measures; **denotes significance of p < 0.001. ‡Indication of significance (p < 0.05) in comparisons proceeding the second minute of PEMI (PEMI2), relevant for validating measures of metaboreflex stimulation.

The majority of VE and RR measures failed to be distributed normally (p < 0.05), thus non-parametric analysis was applied and found significance between at least two stages for VE (p = 0.004, η^2_H = 0.057), but not for RR (p = 0.194). Pairwise comparisons for VE suggest a

significant difference for the HG2 stage (12.1±3.90 L/min.) to the REC2 stage (9.32±3.49 L/min.; $p = 0.016$) only. Table 4.7 displays the group data for these measures during the handgrip and subsequent PEMI testing.

Stages	VE (L/min.)		RR (bpm)	
	Mean	SD (±)	Mean	SD (±)
BL	9.43	2.89	9.60	2.96
HG1	11.2	3.33	10.9	3.82
HG2	12.1	3.90	10.6	3.28
HG3	13.0	4.29	11.3	3.47
PEMI1	11.3	4.27	9.97	3.09
PEMI2	11.3	4.43	9.39	3.28
PEMI3	11.0	3.58	10.6	4.13
REC1	10.0	3.63	9.37	3.25
REC2	9.32	3.49	9.82	3.77
REC3	9.51	3.32	9.68	3.57

Table 4.7. Table detailing the group mean values and corresponding standard deviations (SD) for the ventilation (VE) and respiratory rate (RR) during the handgrip exercise and subsequent post-exercise muscle ischemia (PEMI) testing.

4.3.2 Extracranial and Intracranial Hemodynamic Outcomes

No significant differences were observed when comparing MCAv measures between stages ($F[3.93, 98.24] = 1.401$, $p = 0.24$, generalized $\eta^2 = 0.015$), nor ICAv measures ($F[4.05, 89.14] = 1.836$, $p = 0.128$, generalized $\eta^2 = 0.022$). In terms of ICAd, there were also no significant changes observed between stages in this test ($F[4.56, 95.72] = 1.208$, $p = 0.312$, generalized $\eta^2 = 0.006$). The data for these measures are tabulated below (Table 4.8).

Stages	MCAv (cm/s)		ICAv (cm/s)		ICAd (cm)	
	Mean	SD (±)	Mean	SD (±)	Mean	SD (±)
BL	61.69	10.38	35.24	8.07	0.511	0.072
HG1	62.93	10.50	37.37	8.17	0.504	0.079
HG2	61.48	12.11	37.61	8.40	0.488	0.061
HG3	61.92	13.50	38.05	8.13	0.499	0.074
PEMI1	60.28	13.40	35.13	7.68	0.504	0.079
PEMI2	59.15	12.79	35.24	9.44	0.503	0.080
PEMI3	60.11	13.95	35.46	9.87	0.492	0.087
REC1	61.72	11.64	35.15	8.94	0.492	0.083
REC2	61.54	11.93	34.74	10.17	0.492	0.065
REC3	61.11	12.54	35.03	8.94	0.490	0.075

Table 4.8. Table detailing the group mean values and corresponding standard deviations (SD) for the middle cerebral artery blood flow velocity (MCAv), the internal carotid artery blood flow velocity (ICAv) and the internal carotid artery diameter (ICAd) during the handgrip exercise and subsequent post-exercise muscle ischemia (PEMI) testing.

Extracranial ICA $\dot{\gamma}$ did not show significant changes for any stage comparisons during the handgrip and subsequent PEMI (F[4.45, 97.98] = 1.587, p = 0.178, generalized η^2 = 0.015), nor did the Q_{ICA} (F[3.85, 84.71] = 1.733, p = 0.152, generalized η^2 = 0.018). Given that MCAv and ICAv did not change significantly, these results for ICA $\dot{\gamma}$ and Q_{ICA} are consistent, as the previously described calculations for these measures are derived from direct flow velocity and diameter measures in the ICA. Tabulated group values for ICA $\dot{\gamma}$ and Q_{ICA} during this test are found below (Table 4.9).

Stages	ICA $\dot{\gamma}$ (/s)		Q_{ICA} (mL/min.)	
	Mean	SD (±)	Mean	SD (±)
BL	282.89	80.66	217.94	62.04
HG1	307.51	96.49	222.75	60.52
HG2	311.76	94.42	221.19	66.25
HG3	314.40	90.92	224.13	62.10
PEMI1	288.68	86.12	209.89	61.58
PEMI2	288.89	94.01	210.44	71.31
PEMI3	297.05	94.90	206.54	76.50
REC1	295.86	94.62	203.43	74.52
REC2	289.46	98.92	199.08	74.13
REC3	294.22	91.52	202.41	74.71

Table 4.9. Table detailing the group mean values and corresponding standard deviations (SD) for the internal carotid artery (ICA) shear rate ($\dot{\gamma}$) and the ICA volumetric flow (Q_{ICA}) during the handgrip exercise and subsequent post-exercise muscle ischemia (PEMI) testing.

Figure 4.8 also illustrates the consistency in hemodynamic measures during the handgrip and subsequent PEMI testing; measures of MCAv, ICAv, and ICA $\dot{\gamma}$ are plotted in this figure, where some delineation can be seen between male and female values throughout the test. However, sex-comparative analysis does not indicate any significant sex differences between the variability in MCAv, ICAv, and ICA $\dot{\gamma}$ (p = 1.0, p = 0.983, and p = 0.985, respectively).

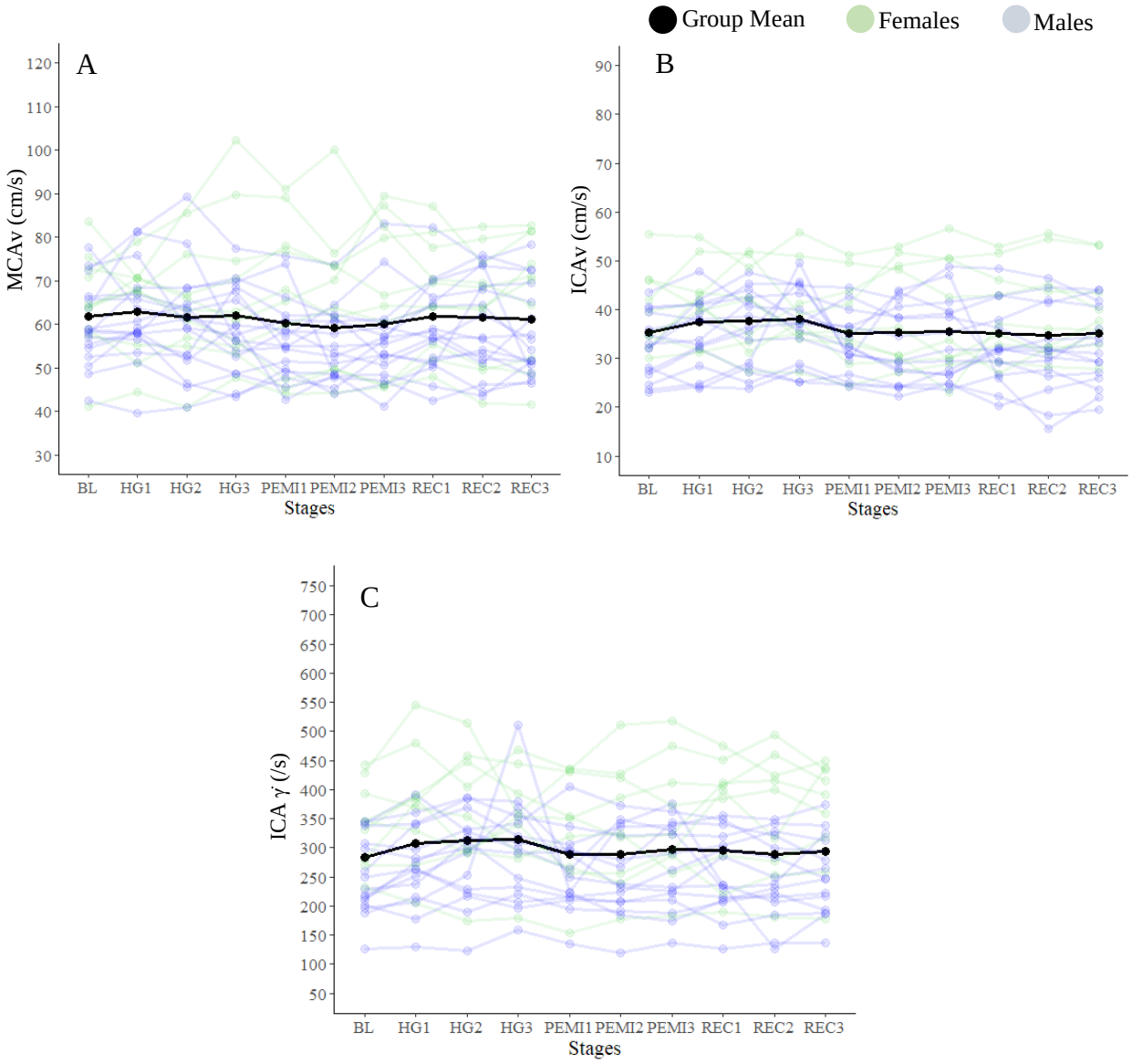

Figure 4.8. Scatterplots illustrating changes in the (A) middle cerebral artery flow velocity (MCAv), the (B) internal carotid artery flow velocity (ICAv), and the (C) internal carotid artery shear rate (ICA $\dot{\gamma}$) during the handgrip exercise and subsequent post-exercise muscle ischemia (PEMI) testing. Group means are represented by the black line, females' values are green, and males' values are blue.

Relevant for the handgrip and subsequent PEMI protocol is the measure of intracranial MCA CVC and CVR change; there was a significant change observed between at least two stage measures for both CVC (F[3.63, 87.02] = 8.174, $p < 0.001$, generalized $\eta^2 = 0.103$) and CVR (F[3.63, 87.08] = 7.647, $p < 0.001$, generalized $\eta^2 = 0.1$). As these measures are inversely related, the significance occurred for the same stage comparisons, wherein the PEMI2 measure

for CVC (0.62±0.15 cm/[mmHg•s]) rose significantly to the REC1 stage (0.70±0.13 cm/[mmHg•s]; $p = 0.014$) and the REC2 stage (0.74±0.17 cm/[mmHg•s]; $p = 0.016$), while CVR decreased from the PEMI2 stage (1.69±0.40 [mmHg•s]/cm) to the REC1 stage (1.47±0.28 [mmHg•s]/cm; $p = 0.007$) and the REC2 stage (1.44±0.36 [mmHg•s]/cm; $p = 0.043$). Tabulated values for CVC and CVR during the handgrip and subsequent PEMI are provided below in Table 4.10.

Stages	CVC (cm/[mmHg•s])		CVR ([mmHg•s]/cm)	
	Mean	SD (±)	Mean	SD (±)
BL	0.72	0.14	1.44	0.28
HG1	0.69	0.12	1.49	0.29
HG2	0.66	0.12	1.57	0.32
HG3	0.64	0.14	1.62	0.34
PEMI1	0.64	0.14	1.65	0.36
PEMI2	0.62	0.15	1.69	0.40
PEMI3	0.65	0.18	1.63	0.41
REC1	0.70‡	0.13	1.47‡	0.28
REC2	0.74‡	0.17	1.44‡	0.36
REC3	0.74	0.18	1.44	0.35

Table 4.10. Table detailing the group mean values and corresponding standard deviations (SD) for the intracranial cerebrovascular conductance (CVC) and cerebrovascular resistance (CVR) during the handgrip exercise and subsequent post-exercise muscle ischemia (PEMI) testing. *Indication of significance in pairwise paired t-test ($p < 0.05$), relative to the initial baseline (BL) measures; **denotes significance of $p < 0.001$. ‡Indication of significance ($p < 0.05$) in comparisons proceeding the second minute of PEMI (PEMI2), relevant for validating measures of metaboreflex stimulation.

4.3.3 Metaboreflex Pulsatility and Damping with Metaboreflex Stimulation

In terms of PI, there was a significant difference observed between at least two measures during this handgrip exercise and subsequent PEMI, both for ICA PI (F[4.47, 93.84] = 3.136, p = 0.015, generalized η^2 = 0.057) and MCA PI (F[4.22, 105.43] = 2.431, p = 0.049, generalized η^2 = 0.041) measures. The significant comparison for ICA PI was seen with the decrease between BL (1.47±0.38) and HG1 (1.31±0.34; p = 0.032), while the increase in MCA PI from PEMI3 (0.81±0.14) to REC1 (0.91±0.16; p = 0.026) was the only significant comparison for the intracranial PI measures. Several of the measures for DFi did not conform with the test for normality, thus the non-parametric analysis suggested that there were no significant comparisons between stages in terms of pulsatile damping (p = 0.89). Values for the group responses in terms of extracranial and intracranial PI, as well as DFi, are tabulated below (Table 4.11).

Stages	ICA PI (ratio)		MCA PI (ratio)		DFi (ratio)	
	Mean	SD (±)	Mean	SD (±)	Mean	SD (±)
BL	1.47	0.38	0.90	0.17	1.63	0.38
HG1	1.31*	0.34	0.88	0.19	1.48	0.38
HG2	1.30	0.45	0.85	0.19	1.51	0.33
HG3	1.21	0.28	0.83	0.17	1.46	0.37
PEMI1	1.34	0.41	0.88	0.20	1.52	0.39
PEMI2	1.27	0.38	0.83	0.17	1.50	0.35
PEMI3	1.31	0.40	0.81	0.14	1.59	0.46
REC1	1.42	0.48	0.91	0.16	1.53	0.42
REC2	1.47	0.43	0.88	0.17	1.62	0.43
REC3	1.39	0.38	0.86	0.19	1.58	0.55

Table 4.11. Table detailing the group mean values and corresponding standard deviations (SD) for the middle cerebral artery pulsatility (MCA PI), the internal carotid artery pulsatility (ICA PI) and the damping factor index (DFi) during the handgrip exercise and subsequent post-exercise muscle ischemia (PEMI). *Indication of significance in pairwise paired t-test ($p < 0.05$), relative to the initial baseline (BL) measures; **denotes significance of $p < 0.001$. ‡Indication of significance ($p < 0.05$) in comparisons proceeding the second minute of PEMI (PEMI2), relevant for validating measures of metaboreflex stimulation.

In Figure 4.9, the DFi response is plotted along with the change scores per timewise stage comparison throughout the test; although there were no significant differences in DFi throughout this test, the variability in DFi responses can be better visualized. Notably, the transition from HG3 to PEMI1 displays a median IQR of 45.7, whereas the rest of the timewise comparisons have a mean IQR of 21.1; this suggests that the variability observed during the handgrip exercise to PEMI transition may not be adequately explained, but that the resultant change in DFi is insignificant on a group level.

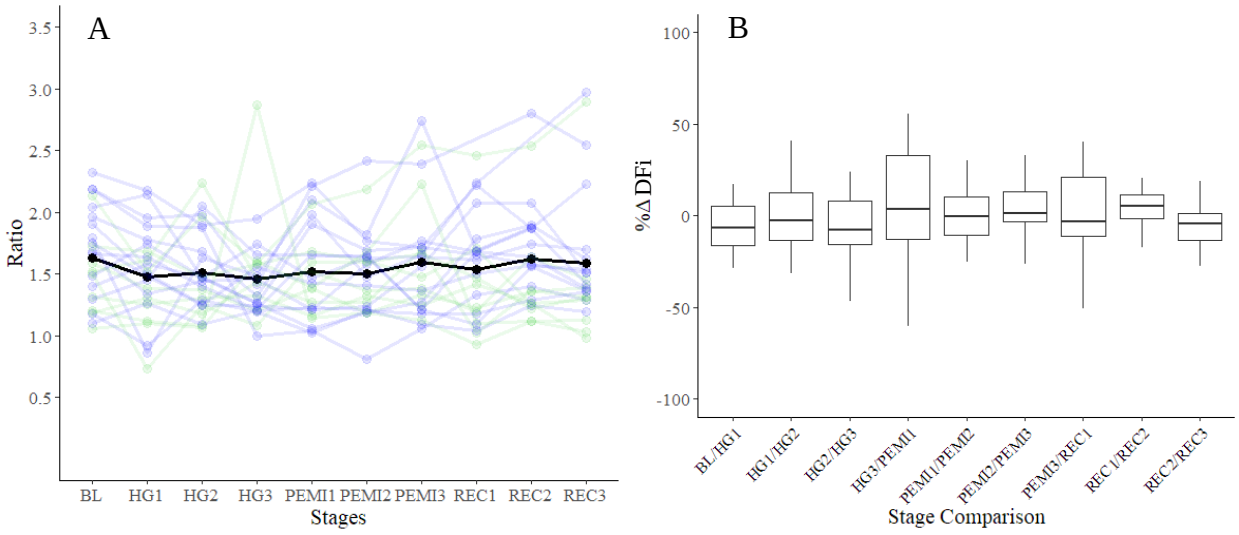

Figure 4.9. Scatterplot (A) and boxplot (B) graphs related to changes in damping factor index (DFi) during the handgrip exercise and subsequent post-exercise muscle ischemia (PEMI) testing: (A) the left panel shows group changes in DFi per stage, where group means are represented by the black line, females' values are green, and males' values are blue; (B) the right panel shows percent change (%Δ) in DFi per stage comparison. The stage comparisons are chronological from the initial baseline (BL) stage to the three minutes of handgrip exercise stages (HG1, HG2, HG3), then into the three minutes of PEMI (PEMI1, PEMI2, PEMI3), and finally to the three minutes of recovery post-occlusion (REC1, REC2, REC3).

4.4 Relating Transient Hypercapnia and PEMI Responses

The assessment of endothelial function by proxy of change in ICAd during the transient hypercapnic breathing test allows for the correlation between the peak diameter %ΔICAd to the DFi observed during handgrip and PEMI; given that the handgrip exercise was intended to reach

fatigue by the final minute, based on piloting the 30% MVC for three minutes, measures at HG3 were used for all participants in comparing against their %ΔICAd during the breathing test. Additionally, the most robust MAP responses to the metaboreflex stimulation occurred from PEMI2, so this value was also used for all participants in comparing against their %ΔICAd during the breathing test. The resultant correlations are plotted below (Figure 4.10): the panel A and C show the negligible and non-significant correlation between %ΔICAd and DFi, as well as %ΔDFi, during HG3 ($r = 0.041$, $p = 0.86$; $r = 0.026$, $p = 0.91$, respectively), while the panels B and D display a weak non-significant positive correlation between measures of %ΔICAd and DFi during PEMI2, as well as %ΔDFi from BL to PEMI2 ($r = 0.35$, $p = 0.11$; $r = 0.34$, $p = 0.12$).

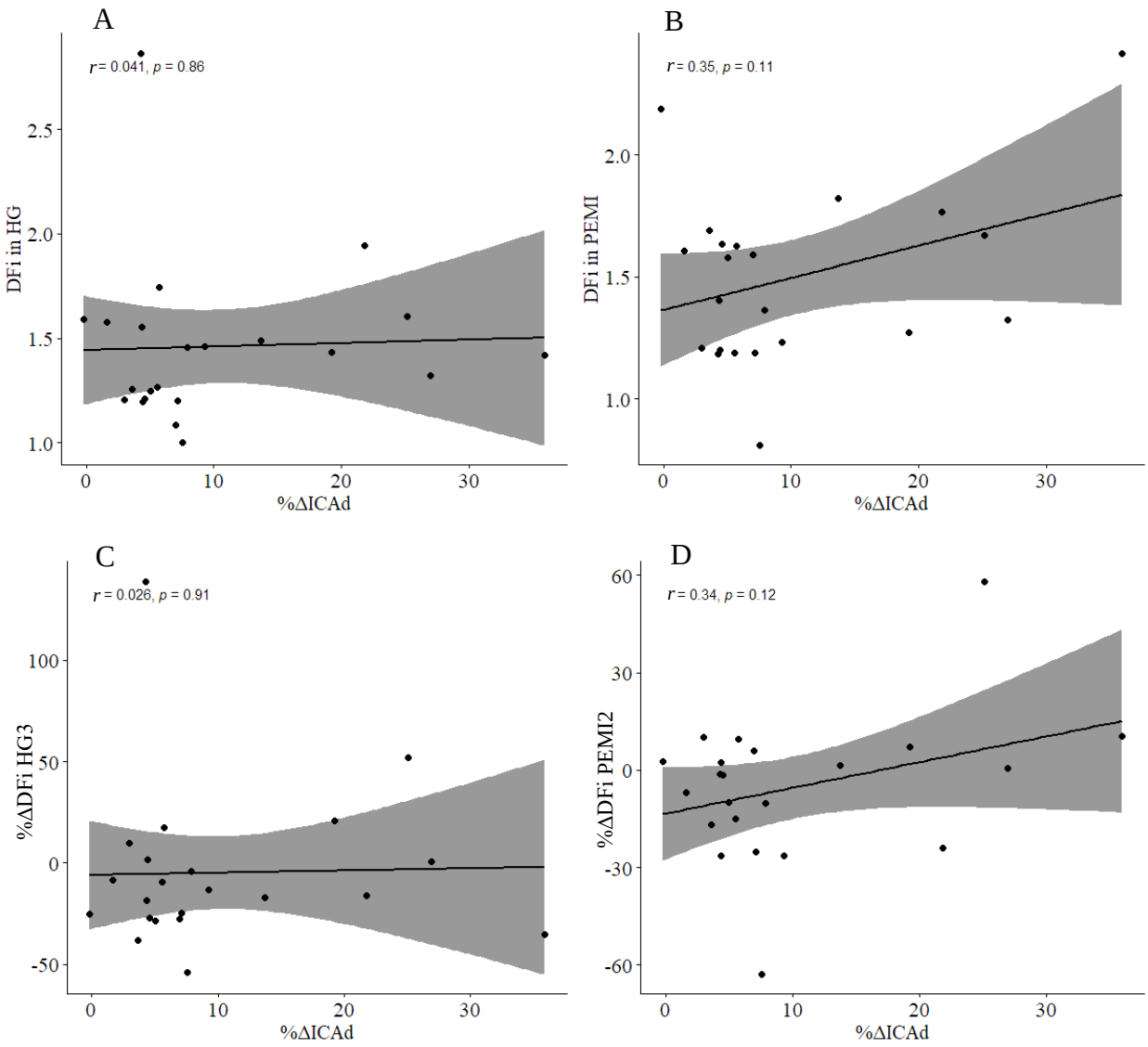

Figure 4.10. Scatterplot graphs plotting the (A, C) correlation between the damping factor index (DFi) against the peak change in ICA diameter (%ΔICAd) during the third minute of handgrip exercise (HG3), both in (A) absolute DFi and (C) relative percent change in DFi (%ΔDFi) from the baseline (BL) measure (n = 22). Additionally, scatterplot graphs plot the (B, C) correlation between the DFi against the peak change in peak %ΔICAd during the second minute of post-exercise muscle ischemia (PEMI2), both in (C) absolute DFi and (D) %ΔDFi from the BL measure (n = 22).

Chapter 5: Discussion and Conclusions

5.1 Summary of the Experimental Outcomes

Current measures of CBF responses to PEMI stimulation often disregard the mechanistic implications of endothelial function in extracranial vasculature. The purpose of this study was to quantify the regulation of cerebrovascular hemodynamics relative to the metaboreflex and arterial shear-mediated vasodilatory stimulation. This thesis also sought to understand if the responses to the metaboreflex stimulation were associated with vasodilatory changes observed during the hypercapnic breathing protocol, in terms of hemodynamics. The aim then was to assess CBF at rest, during a 30-second hypercapnic breathing challenge, during single-limb dynamic fatiguing handgrip exercise, and PEMI with limb occlusion in young and healthy adults. The first hypothesis for this study stated that the cerebrovascular hemodynamic damping at rest would be preserved during handgrip exercise and during subsequent PEMI; the data presented above supports this. The second hypothesis focused on the expected positive relationship between cerebral endothelial responses, indexed by shear-mediated ICA vasodilation to transient CO_2, and the hemodynamic buffering observed during handgrip with subsequent PEMI. However, no significant relationships, positive or negative, were observed between shear-mediated vasodilation and hemodynamic changes during handgrip or PEMI ($p \geq 0.11$). It is worth noting that our transient hypercapnic breathing test did elicit significant vasodilation in response to increases in shear-mediated vasodilation ($p = 0.021$), while PEMI did elicit a significant BP-dependent response to the metaboreflex isolation ($p = 0.005$). The following sections will discuss the primary and secondary findings in more detail.

5.1.1 Inferences for the Proposed Hypotheses

The results support the first hypothesis, wherein during handgrip and subsequent PEMI testing the lack of significant differences in DFi ($p = 0.89$) infers that the damping was conserved when promoting the metaboreflex. The second hypothesis put forth in this thesis study was not completely validated by the statistical analysis, as there was no significant correlation between the degree of shear-mediated vasodilation in the ICA during the transient hypercapnic breathing test, against the absolute DFi observed during handgrip or subsequent PEMI ($p = 0.86$ and $p = 0.11$, respectively). The weak non-significant positive correlation between %ΔICAd and absolute DFi ($r = 0.35$), as well as %ΔDFi ($r = 0.34$, $p = 0.12$), during PEMI is suggestive that there is no relationship to endothelial function when stimulating the metaboreflex; though, comparing to the negligible relationship observed for handgrip, elucidating this the correlation for PEMI measures may require more sampling power for the %ΔICAd (n = 28). These findings suggest consistency with the hypothesized positive impact of the endothelial function on hemodynamic buffering during metaboreflex stimulation when compared to the handgrip responses, though there are not sufficient statistics to support the relationship between endothelial function and DFi during PEMI from this thesis study. To give proper context to all hemodynamic PEMI outcomes, the metaboreflex MAP and HR responses are consistent with the responses in the literature (Fisher et al., 2013); so these results suggest that young and healthy adults do not experience significant damping of hemodynamic stress related to the metaboreflex.

5.1.2 Relating to Cerebrovascular Health

Current literature suggests that cerebral hemodynamic regulation in healthy populations is preserved during exercise (Thomas et al., 2021), whereas chronic disease-states (e.g.,

hypertension, diabetes mellitus, heart failure) may fail to accommodate the increased hemodynamic stress (Reed et al., 2024). Within the healthy sample from this thesis, a lack of significance related to the metaboreflex-altering cerebral pulsatile damping is consistent with this aforementioned literature. This is important because in individuals with impaired damping, where the pulsatile hemodynamic buffering alters significantly during exercise, may be indicative of compromised cerebrovascular compliance that increases the risk for harmful pulsatile transmittance (Mitchell, 2018). Additionally, the presence of chronic disease has been correlated with a loss of metaboreflex function; as sympathetic outflows help to determine the downstream constriction of the vasculature, the abnormal function of the EPR can result in impaired cardiovascular and respiratory function (Teixeira & Vianna, 2022). Whether these disease-states are more causative of the metaboreflex dysfunction, or the impairment of the metaboreflex is a significant risk factor for these disease-states, remains not well understood and requires future experimental investigation. The results of this thesis are unable to provide any relevance to pathological disease-states, however, the findings support that in healthy individuals, the brain is capable of adequately buffering hemodynamic forces during handgrip exercise and metaboreflex stimulation.

Stimulating alterations in hemodynamic buffering may be inherently challenging in healthy populations, as the role of damping is to mitigate harmful pulsatile transmittance, thus preserving brain health. The methodological design of this thesis provided a systemic blood pressure response to both handgrip and metaboreflex stimulation; however, no adverse pulsatile transmittance was observed. In other systemic challenges, autonomic stimulation with sympathetic cold-pressor testing indicates improved damping responses (Lefferts et al., 2021). Additionally, recent work from our CHEERS laboratory suggests that pharmacological

interventions in young and healthy adults can provoke alterations in DFi (Underwood, 2024). Underwood demonstrated mechanistic detection of the factors that drive DFi, wherein after administering cyclooxygenase inhibitors such as indomethacin, an increase in CVR and reduction in DFi is observed. In addition, inotropes such as dobutamine were demonstrated to reduce DFi without CVR changes. This pharmacological alteration in DFi appears to be different depending on altitude: sea level measures suggest that DFi is unchanged with indomethacin, but this is not the same result observed at high altitude (5050 m above sea level); the same altitude dependency occurs for dobutamine, wherein only a significant change in DFi was observed at sea level (Underwood, 2024). Future studies aiming to detect mechanistic regulation of DFi in young and healthy adults should investigate pharmacological and sympathetic-mediated mechanisms. This may give further insight into how DFi may be clinically relevant for assessing the transmittance of pulsatile hemodynamic stress over the adult lifespan and with changing environmental factors.

Pathological arterial stiffening is associated with age and disease and is thought to increase deleterious transmission of vascular hemodynamic forces based on current literature (Mitchell et al., 2011). The outcome of this increased transmission is microvascular damage, that may precede cognitive decline; in other words, attenuated damping across extracranial to intracranial cerebral arteries would be indicative of a harmful transmitted hemodynamic stress if CVR is not sufficiently modulated. As indicators of downstream resistance and conductance in this thesis study, CVC and CVR help demonstrate how the maintenance of damping encompasses changes in downstream resistance, likely to mitigate detrimental flow velocity into the microvasculature. Ultimately, the findings of this thesis suggest that deviations from a healthy cerebral vasculature may provide some prognostic value toward determining cerebrovascular disease risk factors.

Current literature suggests that microvascular damage is associated with decreases in damping factor across cerebrovascular arteries; a resultant increase in perivascular spaces within the basal ganglia has been observed when damping is attenuated, thus increasing the risk factor for cerebral small vessel disease (van den Kerkhof et al., 2023). Additionally, compromises in other measures of conduit vessel stiffness, such as β-stiffness, may be sensitive predictors for cognitive impairment in healthy aging humans (Dubose et al., 2017). With the context of the results herein, a properly powered correlation between the peak %ΔICAd and the ICA $\dot{\gamma}$ AUC may allow for a greater understanding of how these measures of endothelial function in healthy populations have clinical significance when also applied to chronic disease-state populations.

5.1.3 Implications for Assessing Hemodynamic Buffering

The transient hypercapnic breathing protocol was expected to elicit vasodilation in the ICA as a result of increases in shear rate, due to 30 seconds of paced hypercapnic breathing through a Douglas bag, which proceeded two deep breaths. The results for this test supported the notion that the 9% transient CO_2 stimulus was able to elicit shear-mediated vasodilation in the ICA, which corroborates the findings of Hoiland et al. (2022), where blocking eNOS resulted in ~37% decrease in shear-mediated vasodilation. This group also observed ICA shear-mediated vasodilation of ~3.3% during transient hypercapnia with end-tidal forcing, while an adjusted peak %ΔICAd of 5.99±4.33% was observed in this thesis study. Our observed value coincides more with the aforementioned researchers' observations during steady-state hypercapnia (5.3±2.9%) (Hoiland et al., 2017). Although our correlation (r = 0.23) was underpowered for significance (p = 0.3), the positive correlation is indicative of a similar response in terms of endothelial function in the ICA (Hoiland et al., 2017); the correlation adjusted to exclude

extraneous values (outside 95% CI) is strong and significant ($r = 0.86$, $p < 0.001$). As discussed later in the context of study limitations, the extraneous values for this measure are likely a product of inherent challenges in maintaining vessel imaging during dynamic breathing tests, which is detrimental to signal quality and contributed to attrition. In order to properly power this correlation, a *post hoc* ANOVA calculation suggests an n = 34 (one-way ANOVA; partial $\eta^2 = 0.25$, $\alpha = 0.1$, power [1-β] = 0.9, correlation = 0.23); in assessing this correlation, proper sex-comparative measures should be undertaken with an equal number of males and females (n = 17, each).

It is uncertain if the hypocapnia observed during the handgrip and subsequent PEMI protocol confounded the DFi response. The hyperventilation-induced hypocapnia observed in this investigation is expected based on the observation by Braz et al. (2014). Interestingly, given that CVR did not increase, the hypocapnia observed in our study did not result in any significant downstream vasoconstriction. Braz et al. (2014) also demonstrated that by maintaining normocapnia during PEMI, MCAv increased rather than remaining stable. Their findings suggest that PEMI stimulated a neurovascular coupling (NVC) response through afferent feedback from fatiguing muscles, that countered any subsequent hypocapnic vasoconstriction. Our findings corroborate this outcome and despite the lack of significant reduction in CVR, the maintained DFi during HG and PEMI suggest that the afferent feedback from the working muscles does have a role in protecting the brain from deleterious hemodynamic forces. Thus, while we are unable to refute or confirm if confounding vasoconstriction altered the DFi outcomes during the PEMI protocol, the significant return to baseline CVC and CVR values during recovery from PEMI does support some beneficial cerebrovascular and systemic interaction during

metaboreflex stimulation; this may infer hemodynamic buffering between extra and intracranial cerebral vessels during this test.

The lack of association between DFi during the shear-mediated vasodilation and PEMI protocol suggests that, rather than endothelial-mediated DFi regulation, other factors play a role. One prominent mechanistic factor worth investigating in future studies is the impact of myogenic tone on DFi during handgrip and PEMI. Within the current literature, myogenic tone mediated by vSMC is thought to represent an autoregulatory contribution to resistance vessel vasoconstriction during sustained BP challenges (Carlson et al., 2008). The role of MCA and ICA myogenic tone in maintaining damping during the BP-dependent metaboreflex stimulation may be relevant (Jackson, 2021), thus hemodynamic buffering may be preserved by changes in vSMC contribution, despite alterations in cerebrovascular regulation due to the metaboreflex. Overall, given the weak positive correlation between DFi during PEMI and the degree of shear-mediated vasodilation ($r = 0.35$, $p = 0.11$), it is viable to assess these same measures along with a hypocapnic assessment under more dynamically controlled $PetCO_2$ conditions (i.e., end-tidal forcing) and a $PaCO_2$ correction algorithm (Tymko et al., 2016). Future investigations should also aim to inhibit myogenic tone, to assess the role of resistance artery vSMC in maintaining damping during PEMI investigations.

5.2 Limitations

Several considerations must be made in relation to inferences from the results of this research investigation. These considerations will provide beneficial perspectives on how to conduct and reproduce this thesis study's findings in future investigations aiming to quantify the impact of metaboreflex stimulation on cerebral hemodynamics, when also accounting for differences in

endothelial function. One limitation of this study is the impact of hyperventilation-induced hypocapnia. This study used a forced paced-breathing technique in an attempt to mitigate this hyperventilation-induced hypocapnia and the initial goal was to increase ventilation by increasing breathing rate. However, our pilot work indicated that controlling breathing rate at 7.5 bpm during the hypercapnic breathing test resulted in more optimum increases in VE potentially due to increased tidal volume, rather than breathing rate, which increases the influence of physiological dead space (West, 1971).

Unfortunately, the lower breathing rate during handgrip exercise was reported to be a challenge for the majority of participants, as they indicated that timing breathing whilst performing cyclical hand gripping was difficult. This handgrip exercise which resulted in sustained hypocapnia into the PEMI stages may have had a confounding vasoconstriction of ~2%, given the proposed 3.2±5.3% vasoconstriction observed by Willie et al. (2012) from a $PaCO_2$ of 40 mmHg (normocapnic) to 30 mmHg (hypocapnic). In regard to addressing the influence of hypocapnic vasoconstriction on hemodynamic outcomes in this study, considering a volumetric damping approach may have provided more insight into the effect of these confounding variables; thus, the ability to compare *Q* between the ICA to MCA is pertinent. As aforementioned, MCA vessel diameter measures were recorded, but were unable to be analyzed due to current software limitations. Future investigations should employ end-tidal forced systems for clamping $PetCO_2$, while employing accurate measures of MCA diameter to infer volumetric flow changes during similar testing to this thesis study.

As rationalized, the two deep breaths preceding the transient 30-second Douglas bag breathing were done based on piloting the degree of stimulus-response; however, this method may introduce an underestimation of $PaCO_2$ with $PetCO_2$ during this test, as current literature

suggests that a lower RR (~6 bpm) alters the gradient between $PaCO_2$ to $PetCO_2$ (Ito et al., 2008; Tymko et al., 2016). In reality, the ~21 mmHg change in $PetCO_2$ between BL2 and CO2 stages may represent a ~15 mmHg change in $PaCO_2$, based on the current research and methodological considerations. Also of note, as only an RR of 7.5 bpm was assessed, this study is limited by the ability to corroborate differences in cardiorespiratory responses with differing RR. That said, during the handgrip portion of the testing the RR of 7.5 bpm may have made the $PaCO_2$ to $PetCO_2$ gradient more comparable, as the literature has also described a compounding overestimation during exercise (Jones et al., 1979; Robbins et al., 1990). This methodology remains a limitation though, as the impact of hypocapnia on the hemodynamic measures during this test means that more accurately estimating $PaCO_2$ is irrelevant if hemodynamic outcomes are limited in accuracy. Additionally, the aforementioned lost stage measures for ICA outcomes during the hypercapnic breathing test are related to the difficulty in maintaining accurate ultrasound signal quality during this test. This study does appear to be underpowered for the proper correlation between ICA $\dot{\gamma}$ AUC and %ΔICAd; the attrition to scanner error resulted in an already underpowered sample size for ICA measures (n = 22), which was coupled with the extraneous and possibly erroneous values that resulted from scanner instability. During ultrasound scanning of the ICA, the dynamic changes in breathing or drive to swallow are challenging to account for and often result in the vessel image being altered; resultant changes in the scanning angle or probe repositioning can impact the measures of diameter during this test. Therefore, future research in this area should consider having more explicit control of possible differences in $PaCO_2$ to $PetCO_2$, whilst accounting for a greater participant attrition due to data collection difficulty.

Female sex hormones may be important modulators of cerebrovascular disease over the adult lifespan (Bushnell et al., 2014; Li & Singh, 2014; Tarumi et al., 2014), thus ignoring sex-comparative research in this field is contrary to a complete mechanistic understanding of healthy cerebrovascular regulation. In this thesis study, neither the menstrual cycle nor sex hormone levels were controlled for, and the sex-based group distributions were heterogenous (i.e., 17 Males versus 11 females). The initial power calculation required homogenous group distribution (13 males; 13 females) in order to detect meaningful differences; thus, this thesis study was underpowered to specifically interpret any sex-based outcomes. Within-group female hemodynamic variability was greater compared to males, which is likely explained by the inability to account for female variability due to sex hormone variance over the menstrual cycle in this thesis study. Possible differences in male and female pulsatility have been observed in the literature (Alwatban et al., 2021; Lefferts et al., 2023), along with some contradicting data to suggest that the decline in estrogen following menopause may (Guo et al., 2023; Lefferts et al., 2020) or may not (Ruediger et al., 2023) be related to age-related declines in cerebrovascular regulation (Koep et al., 2023). Estrogen is understood in the literature to play an important role in regulating the vascular tone (Mendelsohn & Karas, 1999; Miller & Duckles, 2008), but cerebrovascular implications are currently vague and difficult to characterize (Ruediger et al., 2021). This thesis study was limited in the ability to draw meaningful physiological differences between biological males and females, but future investigations of hemodynamic responses to endothelial function and metaboreflex stimulation should employ an equal number of biological male and female participants, whilst accounting for differences in sex hormone levels.

5.3 Conclusion

Using ultrasound techniques, this thesis study supported the notion that pulsatile cerebral hemodynamic damping between extracranial ICA and intracranial MCA did not change during metaboreflex stimulation, using a submaximal dynamic handgrip protocol that preceded PEMI. Despite significant reflexive increases in MAP and HR during HG, and MAP during PEMI, neither the responses during the handgrip exercise fatigue nor peak PEMI responses were effective at altering the DFi response in young and healthy adults. Endothelial function during the hypercapnic breathing test successfully displayed shear-mediated vasodilatory responses to the transient 9% CO_2 Douglas bag breathing protocol. The promotion of shear-mediated vasodilation via this method may provide a reproducible test to increase $PaCO_2$ transiently, though scanner instability during hypercapnic breathing tests presents a challenge for quality data acquisition. Though this thesis study was likely underpowered for the correlation between endothelial function to the degree of damping during PEMI, the weak positive correlation may be better elucidated by research that also assesses changes in myogenic tone and hypocapnic vasoconstriction. Future investigations should be powered to understand these implications properly, while also focusing on other probable mechanisms of hemodynamic regulation, such as the aforementioned myogenic tone of the MCA and ICA. Additionally, these investigations should account for differing sex hormone levels and the role of chronic disease-states, in order to strive for a greater understanding of how exercise-dependent mechanisms may have a role in healthy CBF regulation.

References

Aaslid, R., Markwalder, T. M., & Nornes, H. (1982). Noninvasive transcranial Doppler ultrasound recording of flow velocity in basal cerebral arteries. *J Neurosurg*, *57*(6), 769-774. https://doi.org/10.3171/jns.1982.57.6.0769

Ainslie, P. N., Ashmead, J. C., Ide, K., Morgan, B. J., & Poulin, M. J. (2005). Differential responses to CO2 and sympathetic stimulation in the cerebral and femoral circulations in humans. *The Journal of Physiology*, *566*(2), 613-624. https://doi.org/https://doi.org/10.1113/jphysiol.2005.087320

Ainslie, P. N., & Duffin, J. (2009). Integration of cerebrovascular CO2 reactivity and chemoreflex control of breathing: mechanisms of regulation, measurement, and interpretation. *American Journal of Physiology-Regulatory, Integrative and Comparative Physiology*, *296*(5), R1473-R1495. https://doi.org/10.1152/ajpregu.91008.2008

Ainslie, P. N., Murrell, C., Peebles, K., Swart, M., Skinner, M. A., Williams, M. J. A., & Taylor, R. D. (2007). Early morning impairment in cerebral autoregulation and cerebrovascular CO2 reactivity in healthy humans: relation to endothelial function. *Experimental Physiology*, *92*(4), 769-777. https://doi.org/10.1113/expphysiol.2006.036814

Alam, M., & Smirk, F. H. (1937). Observations in man upon a blood pressure raising reflex arising from the voluntary muscles. *J Physiol*, *89*(4), 372-383. https://doi.org/10.1113/jphysiol.1937.sp003485

Alwatban, M. R., Aaron, S. E., Kaufman, C. S., Barnes, J. N., Brassard, P., Ward, J. L.,…Billinger, S. A. (2021). Effects of age and sex on middle cerebral artery blood velocity and flow pulsatility index across the adult lifespan. *Journal of Applied Physiology*, *130*(6), 1675-1683. https://doi.org/10.1152/japplphysiol.00926.2020

Amann, M., Blain, G. M., Proctor, L. T., Sebranek, J. J., Pegelow, D. F., & Dempsey, J. A. (2011). Implications of group III and IV muscle afferents for high-intensity endurance exercise performance in humans. *The Journal of Physiology*, *589*(21), 5299-5309. https://doi.org/10.1113/jphysiol.2011.213769

Amann, M., Sidhu, S. K., Weavil, J. C., Mangum, T. S., & Venturelli, M. (2015). Autonomic responses to exercise: Group III/IV muscle afferents and fatigue. *Autonomic Neuroscience*, *188*, 19-23. https://doi.org/10.1016/j.autneu.2014.10.018

Amann, M., Venturelli, M., Ives, S. J., Morgan, D. E., Gmelch, B., Witman, M. A. H.,…Richardson, R. S. (2014). Group III/IV muscle afferents impair limb blood in patients with chronic heart failure. *International Journal of Cardiology*, *174*(2), 368-375. https://doi.org/10.1016/j.ijcard.2014.04.157

Anderson, T. J., Uehata, A., Gerhard, M. D., Meredith, I. T., Knab, S., Delagrange, D.,…Selwyn, A. P. (1995). Close relation of endothelial function in the human coronary and peripheral circulations. *Journal of the American College of Cardiology*, *26*(5), 1235-1241. https://doi.org/https://doi.org/10.1016/0735-1097(95)00327-4

Armstrong, R. A. (2014). When to use the Bonferroni correction. *Ophthalmic and Physiological Optics*, *34*(5), 502-508. https://doi.org/10.1111/opo.12131

Bonferroni, C. E. (1936). Teoria statistica delle classi e calcolo delle probabilit `a. *Pubblicazioni del R Istituto Superiore di Scienze Economiche e Commerciali di Firenze*, *8*.

Boulton, D., Taylor, C. E., Green, S., & Macefield, V. G. (2018). The metaboreflex does not contribute to the increase in muscle sympathetic nerve activity to contracting muscle during static exercise in humans. *J Physiol*, *596*(6), 1091-1102. https://doi.org/10.1113/jp275526

Boushel, R. (2010). Muscle metaboreflex control of the circulation during exercise. *Acta Physiologica*, *199*(4), 367-383. https://doi.org/10.1111/j.1748-1716.2010.02133.x

Brassard, P., Roy, M.-A., Burma, J. S., Labrecque, L., & Smirl, J. D. (2023). Quantification of dynamic cerebral autoregulation: welcome to the jungle! *Clinical Autonomic Research*, *33*(6), 791-810. https://doi.org/10.1007/s10286-023-00986-2

Braz, I. D., Scott, C., Simpson, L. L., Springham, E. L., Tan, B. W. L., Balanos, G. M., & Fisher, J. P. (2014). Influence of muscle metaboreceptor stimulation on middle cerebral artery blood velocity in humans. *Experimental Physiology*, *99*(11), 1478-1487. https://doi.org/10.1113/expphysiol.2014.081687

Bushnell, C., Mccullough, L. D., Awad, I. A., Chireau, M. V., Fedder, W. N., Furie, K. L.,…Walters, M. R. (2014). Guidelines for the Prevention of Stroke in Women. *Stroke*, *45*(5), 1545-1588. https://doi.org/10.1161/01.str.0000442009.06663.48

Carlson, B. E., Arciero, J. C., & Secomb, T. W. (2008). Theoretical model of blood flow autoregulation: roles of myogenic, shear-dependent, and metabolic responses. *Am J Physiol Heart Circ Physiol*, *295*(4), H1572-1579. https://doi.org/10.1152/ajpheart.00262.2008

Carr, J. M. J. R., Hoiland, R. L., Caldwell, H. G., Coombs, G. B., Howe, C. A., Tremblay, J. C.,…Ainslie, P. N. (2020). Internal carotid and brachial artery shear-dependent vasodilator function in young healthy humans. *The Journal of Physiology*, *598*(23), 5333-5350. https://doi.org/10.1113/jp280369

Carter, H. H., Atkinson, C. L., Heinonen, I. H. A., Haynes, A., Robey, E., Smith, K. J.,…Green, D. J. (2016). Evidence for Shear Stress–Mediated Dilation of the Internal Carotid Artery

in Humans. *Hypertension*, *68*(5), 1217-1224. https://doi.org/10.1161/hypertensionaha.116.07698

Charakida, M., Masi, S., Luscher, T. F., Kastelein, J. J. P., & Deanfield, J. E. (2010). Assessment of atherosclerosis: the role of flow-mediated dilatation. *European Heart Journal*, *31*(23), 2854-2861. https://doi.org/10.1093/eurheartj/ehq340

Claassen, J., Thijssen, D. H. J., Panerai, R. B., & Faraci, F. M. (2021). Regulation of cerebral blood flow in humans: physiology and clinical implications of autoregulation. *Physiol Rev*, *101*(4), 1487-1559. https://doi.org/10.1152/physrev.00022.2020

Cohen, J. (1988). Statistical Power Analysis for the Behavioral Sciences. https://doi.org/10.4324/9780203771587

Costa, F., & Biaggioni, I. (1994). Role of adenosine in the sympathetic activation produced by isometric exercise in humans. *Journal of Clinical Investigation*, *93*(4), 1654-1660. https://doi.org/10.1172/jci117147

Da Silva, G., Da Silva, M., Nascimento, D., Lima Silva, E., Gouvêa, F., De França Lopes, L.,…De Queiroz, T. (2021). Nitric Oxide as a Central Molecule in Hypertension: Focus on the Vasorelaxant Activity of New Nitric Oxide Donors. *Biology*, *10*(10), 1041. https://doi.org/10.3390/biology10101041

Delaney, E. P., Greaney, J. L., Edwards, D. G., Rose, W. C., Fadel, P. J., & Farquhar, W. B. (2010). Exaggerated sympathetic and pressor responses to handgrip exercise in older hypertensive humans: role of the muscle metaboreflex. *American Journal of Physiology-Heart and Circulatory*

Physiology, *299*(5), H1318-H1327. https://doi.org/10.1152/ajpheart.00556.2010

Dinno, A. (2015). Nonparametric Pairwise Multiple Comparisons in Independent Groups using Dunn's Test. *The Stata Journal: Promoting communications on statistics and Stata*, *15*(1), 292-300. https://doi.org/10.1177/1536867x1501500117

Dipla, K., Papadopoulos, S., Zafeiridis, A., Kyparos, A., Nikolaidis, M. G., & Vrabas, I. S. (2013). Determinants of muscle metaboreflex and involvement of baroreflex in boys and young men. *European Journal of Applied Physiology*, *113*(4), 827-838. https://doi.org/10.1007/s00421-012-2493-7

Drew, R. C., Bell, M. P. D., & White, M. J. (2008). Modulation of spontaneous baroreflex control of heart rate and indexes of vagal tone by passive calf muscle stretch during graded metaboreflex activation in humans. *Journal of Applied Physiology*, *104*(3), 716-723. https://doi.org/10.1152/japplphysiol.00956.2007

Dubose, L. E., Voss, M. W., Weng, T. B., Kent, J. D., Dubishar, K. M., Lane-Cordova, A.,…Pierce, G. L. (2017). Carotid β-stiffness index is associated with slower processing speed but not working memory or white matter integrity in healthy middle-aged/older adults. *Journal of Applied Physiology*, *122*(4), 868-876. https://doi.org/10.1152/japplphysiol.00769.2016

Dunn, O. J. (1964). Multiple Comparisons Using Rank Sums. *Technometrics*, *6*(3), 241-252. https://doi.org/10.1080/00401706.1964.10490181

Einthoven, W. (1912). The different forms of the human electrocardiogram and their signification. *The Lancet*, *179*(4622), 853-861. https://doi.org/https://doi.org/10.1016/S0140-6736(00)50560-1

Fisher, J. P., Adlan, A. M., Shantsila, A., Secher, J. F., Sørensen, H., & Secher, N. H. (2013). Muscle metaboreflex and autonomic regulation of heart rate in humans. *The Journal of Physiology*, *591*(15), 3777-3788. https://doi.org/10.1113/jphysiol.2013.254722

Fisher, J. P., Bell, M. P., & White, M. J. (2005). Cardiovascular responses to human calf muscle stretch during varying levels of muscle metaboreflex activation. *Exp Physiol*, *90*(5), 773-781. https://doi.org/10.1113/expphysiol.2005.030577

Fisher, J. P., Young, C. N., & Fadel, P. J. (2015). Autonomic Adjustments to Exercise in Humans. In *Comprehensive Physiology* (pp. 475-512). https://doi.org/https://doi.org/10.1002/cphy.c140022

Fisslthaler, Dimmeler, Hermann, Busse, & Fleming. (2000). Phosphorylation and activation of the endothelial nitric oxide synthase by fluid shear stress. *Acta Physiologica Scandinavica*, *168*(1), 81-88. https://doi.org/https://doi.org/10.1046/j.1365-201x.2000.00627.x

Gao, Z., Henig, O., Kehoe, V., Sinoway, L. I., & Li, J. (2006). Vanilloid type 1 receptor and the acid-sensing ion channel mediate acid phosphate activation of muscle afferent nerves in rats. *J Appl Physiol (1985)*, *100*(2), 421-426. https://doi.org/10.1152/japplphysiol.00659.2005

Gonzalez-Alonso, J., Dalsgaard, M. K., Osada, T., Volianitis, S., Dawson, E. A., Yoshiga, C. C., & Secher, N. H. (2004). Brain and central haemodynamics and oxygenation during maximal exercise in humans. *Journal of Physiology-London*, *557*(1), 331-342. https://doi.org/10.1113/jphysiol.2004.060574

Goodwin, G. M., McCloskey, D. I., & Mitchell, J. H. (1972). Cardiovascular and respiratory responses to changes in central command during isometric exercise at constant muscle

tension. *The Journal of Physiology*, *226*(1), 173-190. https://doi.org/https://doi.org/10.1113/jphysiol.1972.sp009979

Green, D. J., Jones, H., Thijssen, D., Cable, N. T., & Atkinson, G. (2011). Flow-Mediated Dilation and Cardiovascular Event Prediction. *Hypertension*, *57*(3), 363-369. https://doi.org/10.1161/hypertensionaha.110.167015

Guo, W., Wang, X., Chen, Y., Wang, F., Qiu, J., & Lu, W. (2023). Effect of Menopause Status on Brain Perfusion Hemodynamics. *Stroke*. https://doi.org/10.1161/strokeaha.123.044841

Guyenet, P. G. (2014). Regulation of Breathing and Autonomic Outflows by Chemoreceptors. *Comprehensive Physiology*, 1511-1562. https://doi.org/10.1002/cphy.c140004

Hellstrom, G., & Wahlgren, N. G. (1993). Physical exercise increases middle cerebral artery blood flow velocity. *Neuro Surgical Review*, *16*(2), 151-156. https://doi.org/10.1007/bf00258249

Hoiland, R. L., Caldwell, H. G., Carr, J. M. J. R., Howe, C. A., Stacey, B. S., Dawkins, T.,…Ainslie, P. N. (2022). Nitric oxide contributes to cerebrovascular shear-mediated dilatation but not steady-state cerebrovascular reactivity to carbon dioxide. *The Journal of Physiology*, *600*(6), 1385-1403. https://doi.org/https://doi.org/10.1113/JP282427

Hoiland, R. L., Howe, C. A., Coombs, G. B., & Ainslie, P. N. (2018). Ventilatory and cerebrovascular regulation and integration at high-altitude. *Clinical Autonomic Research*, *28*(4), 423-435. https://doi.org/10.1007/s10286-018-0522-2

Hoiland, R. L., Smith, K. J., Carter, H. H., Lewis, N. C. S., Tymko, M. M., Wildfong, K. W.,…Ainslie, P. N. (2017). Shear-mediated dilation of the internal carotid artery occurs independent of hypercapnia. *American Journal of Physiology-Heart and Circulatory Physiology*, *313*(1), H24-H31. https://doi.org/10.1152/ajpheart.00119.2017

Ichinose, M., Saito, M., Kondo, N., & Nishiyasu, T. (2008). Baroreflex and Muscle Metaboreflex: Control of Muscle Sympathetic Nerve Activity. *Medicine & Science in Sports & Exercise*, *40*(12).

Ito, S., Mardimae, A., Han, J., Duffin, J., Wells, G., Fedorko, L.,…Fisher, J. A. (2008). Non-invasive prospective targeting of arterial P(CO2) in subjects at rest. *J Physiol*, *586*(15), 3675-3682. https://doi.org/10.1113/jphysiol.2008.154716

Jackson, W. F. (2021). Myogenic Tone in Peripheral Resistance Arteries and Arterioles: The Pressure Is On! *Frontiers in Physiology*, *12*. https://doi.org/10.3389/fphys.2021.699517

Jafari, M., & Ansari-Pour, N. (2019). Why, When and How to Adjust Your P Values? *Cell J*, *20*(4), 604-607. https://doi.org/10.22074/cellj.2019.5992

Jarvis, S. S., VanGundy, T. B., Galbreath, M. M., Shibata, S., Okazaki, K., Reelick, M. F.,…Fu, Q. (2011). Sex differences in the modulation of vasomotor sympathetic outflow during static handgrip exercise in healthy young humans. *American Journal of Physiology-Regulatory, Integrative and Comparative Physiology*, *301*(1), R193-R200. https://doi.org/10.1152/ajpregu.00562.2010

Jones, N. L., Robertson, D. G., & Kane, J. W. (1979). Difference between end-tidal and arterial PCO2 in exercise. *J Appl Physiol Respir Environ Exerc Physiol*, *47*(5), 954-960. https://doi.org/10.1152/jappl.1979.47.5.954

Jorgensen, L. G., Perko, G., Payne, G., & Secher, N. H. (1993). Effect of limb anesthesia on middle cerebral response to handgrip. *American Journal of Physiology-Heart and Circulatory Physiology*, *264*(2), H553-H559. https://doi.org/10.1152/ajpheart.1993.264.2.H553

Jorgensen, L. G., Perko, G., & Secher, N. H. (1992). Regional cerebral artery mean flow velocity and blood flow during dynamic exercise in humans. *Journal of Applied Physiology*, *73*(5), 1825-1830. https://doi.org/10.1152/jappl.1992.73.5.1825

Jorgensen, L. G., Perko, M., Hanel, B., Schroeder, T. V., & Secher, N. H. (1992). Middle cerebral artery flow velocity and blood flow during exercise and muscle ischemia in humans. *Journal of Applied Physiology*, *72*(3), 1123-1132. https://doi.org/10.1152/jappl.1992.72.3.1123

Kniffki, K. D., Mense, S., & Schmidt, R. F. (1978). Responses of group IV afferent units from skeletal muscle to stretch, contraction and chemical stimulation. *Exp Brain Res*, *31*(4), 511-522. https://doi.org/10.1007/bf00239809

Koep, J. L., Bond, B., Barker, A. R., Ruediger, S. L., Pizzey, F. K., Coombes, J. S., & Bailey, T. G. (2023). Sex modifies the relationship between age and neurovascular coupling in healthy adults. *Journal of Cerebral Blood Flow & Metabolism*, *43*(8), 1254-1266. https://doi.org/10.1177/0271678X231167753

Kruskal, W. H., & Wallis, W. A. (1952). Use of Ranks in One-Criterion Variance Analysis. *Journal of the American Statistical Association*, *47*(260), 583-621. https://doi.org/10.1080/01621459.1952.10483441

Laginestra, F. G., Favaretto, T., Giuriato, G., Martignon, C., Barbi, C., Pedrinolla, A.,…Venturelli, M. (2023). Concurrent metaboreflex activation increases chronotropic and ventilatory responses to passive leg movement without sex-related differences. *European Journal of Applied Physiology*, *123*(8), 1751-1762. https://doi.org/10.1007/s00421-023-05186-4

Lakens, D. (2013). Calculating and reporting effect sizes to facilitate cumulative science: a practical primer for t-tests and ANOVAs. *Frontiers in Psychology*, *4*. https://doi.org/10.3389/fpsyg.2013.00863

Lambert, E. V. (2005). Complex systems model of fatigue: integrative homoeostatic control of peripheral physiological systems during exercise in humans. *British Journal of Sports Medicine*, *39*(1), 52-62. https://doi.org/10.1136/bjsm.2003.011247

Lanfranchi, P. A., & Somers, V. K. (2002). Arterial baroreflex function and cardiovascular variability: interactions and implications. *American Journal of Physiology-Regulatory, Integrative and Comparative Physiology*, *283*(4), R815-R826. https://doi.org/10.1152/ajpregu.00051.2002

Lefferts, W. K., Deblois, J. P., Augustine, J. A., Keller, A. P., & Heffernan, K. S. (2020). Age, sex, and the vascular contributors to cerebral pulsatility and pulsatile damping. *Journal of Applied Physiology*, *129*(5), 1092-1101. https://doi.org/10.1152/japplphysiol.00500.2020

Lefferts, W. K., Lefferts, E. C., Hibner, B. A., Smith, K. J., & Fernhall, B. (2021). Impact of acute changes in blood pressure and arterial stiffness on cerebral pulsatile haemodynamics in young and middle-aged adults. *Exp Physiol*, *106*(7), 1643-1653. https://doi.org/10.1113/ep089319

Lefferts, W. K., Reed, K. S., Rosonke, R. E., Augustine, J. A., & Moreau, K. L. (2023). Age-associated increases in middle cerebral artery pulsatility differ between men and women. *Am J Physiol Heart Circ Physiol*, *325*(5), H1118-h1125. https://doi.org/10.1152/ajpheart.00453.2023

Li, J., Gao, Z., Kehoe, V., Xing, J., King, N., & Sinoway, L. (2008). Interstitial adenosine triphosphate modulates muscle afferent nerve–mediated pressor reflex. *Muscle & Nerve*, *38*(2), 972-977. https://doi.org/10.1002/mus.21014

Li, R., & Singh, M. (2014). Sex differences in cognitive impairment and Alzheimer's disease. *Frontiers in Neuroendocrinology*, *35*(3), 385-403. https://doi.org/10.1016/j.yfrne.2014.01.002

Lis, A., Paleczny, B., & Ponikowska, B. (2021). Understanding mechanoreflex and metaboreflex interactions – a great challenge. *Indian Journal of Physiology and Pharmacology*, *65*(1), 1-11. https://doi.org/10.25259/IJPP_73_2021

Magistretti, P. J., & Allaman, I. (2015). A cellular perspective on brain energy metabolism and functional imaging. *Neuron*, *86*(4), 883-901. https://doi.org/10.1016/j.neuron.2015.03.035

Mavroudis, C. D., Ko, T., Volk, L. E., Smood, B., Morgan, R. W., Lynch, J. M.,…Kilbaugh, T. J. (2022). Does supply meet demand? A comparison of perfusion strategies on cerebral metabolism in a neonatal swine model. *J Thorac Cardiovasc Surg*, *163*(1), e47-e58. https://doi.org/10.1016/j.jtcvs.2020.12.005

Mendelsohn, M. E., & Karas, R. H. (1999). The protective effects of estrogen on the cardiovascular system. *N Engl J Med*, *340*(23), 1801-1811. https://doi.org/10.1056/nejm199906103402306

Miller, V. M., & Duckles, S. P. (2008). Vascular actions of estrogens: functional implications. *Pharmacol Rev*, *60*(2), 210-241. https://doi.org/10.1124/pr.107.08002

Mitchell, G. F. (2018). Aortic stiffness, pressure and flow pulsatility, and target organ damage. *Journal of Applied Physiology*, *125*(6), 1871-1880. https://doi.org/10.1152/japplphysiol.00108.2018

Mitchell, G. F., Van Buchem, M. A., Sigurdsson, S., Gotal, J. D., Jonsdottir, M. K., Kjartansson, Ó.,…Launer, L. J. (2011). Arterial stiffness, pressure and flow pulsatility and brain structure and function: the Age, Gene/Environment Susceptibility – Reykjavik Study. *Brain*, *134*(11), 3398-3407. https://doi.org/10.1093/brain/awr253

Mitchell, J. H., Kaufman, M. P., & Iwamoto, G. A. (1983). The Exercise Pressor Reflex: Its Cardiovascular Effects, Afferent Mechanisms, and Central Pathways. *Annual Review of Physiology*, *45*(1), 229-242. https://doi.org/10.1146/annurev.ph.45.030183.001305

Moraine, J. J., Lamotte, M., Berré, J., Niset, G., Leduc, A., & Naeije, R. (1993). Relationship of middle cerebral artery blood flow velocity to intensity during dynamic exercise in normal subjects. *Eur J Appl Physiol Occup Physiol*, *67*(1), 35-38. https://doi.org/10.1007/bf00377701

Murphy, M. N., Mizuno, M., Mitchell, J. H., & Smith, S. A. (2011). Cardiovascular regulation by skeletal muscle reflexes in health and disease. *Am J Physiol Heart Circ Physiol*, *301*(4), H1191-1204. https://doi.org/10.1152/ajpheart.00208.2011

Nabel, E. G., Selwyn, A. P., & Ganz, P. (1990). Large coronary arteries in humans are responsive to changing blood flow: An endothelium-dependent mechanism that fails in patients with atherosclerosis. *Journal of the American College of Cardiology*, *16*(2), 349-356. https://doi.org/https://doi.org/10.1016/0735-1097(90)90584-C

Nahm, F. S. (2016). Nonparametric statistical tests for the continuous data: the basic concept and the practical use. *Korean Journal of Anesthesiology*, *69*(1), 8. https://doi.org/10.4097/kjae.2016.69.1.8

Ng, A. V., Callister, R., Johnson, D. G., & Seals, D. R. (1994). Sympathetic neural reactivity to stress does not increase with age in healthy humans. *Am J Physiol*, *267*(1 Pt 2), H344-353. https://doi.org/10.1152/ajpheart.1994.267.1.H344

Nobrega, A. C. L., O'Leary, D., Silva, B. M., Marongiu, E., Piepoli, M. F., & Crisafulli, A. (2014). Neural Regulation of Cardiovascular Response to Exercise: Role of Central Command and Peripheral Afferents. *BioMed Research International*, *2014*, 1-20. https://doi.org/10.1155/2014/478965

O'Leary, D. S. (1993). Autonomic mechanisms of muscle metaboreflex control of heart rate. *Journal of Applied Physiology*, *74*(4), 1748-1754. https://doi.org/10.1152/jappl.1993.74.4.1748

Oglat, A. A., Matjafri, M. Z., Suardi, N., Oqlat, M. A., Abdelrahman, M. A., & Oqlat, A. A. (2018). A Review of Medical Doppler Ultrasonography of Blood Flow in General and Especially in Common Carotid Artery. *J Med Ultrasound*, *26*(1), 3-13. https://doi.org/10.4103/jmu.jmu_11_17

Ogoh, S. (2024). Cardiac output-mediated regulation of cerebral blood flow during exercise: Clinical perspectives on the indirect impact of muscle metaboreflex. *Experimental Physiology*. https://doi.org/10.1113/ep091591

Ogoh, S., & Ainslie, P. N. (2009). Cerebral blood flow during exercise: mechanisms of regulation. *Journal of Applied Physiology*, *107*(5), 1370-1380. https://doi.org/10.1152/japplphysiol.00573.2009

Ogoh, S., Sato, K., Hirasawa, A., & Sadamoto, T. (2019). The effect of muscle metaboreflex on the distribution of blood flow in cerebral arteries during isometric exercise. *The Journal of Physiological Sciences*, *69*(2), 375-385. https://doi.org/10.1007/s12576-018-0653-1

Olejnik, S., & Algina, J. (2003). Generalized eta and omega squared statistics: measures of effect size for some common research designs. *Psychol Methods*, *8*(4), 434-447. https://doi.org/10.1037/1082-989x.8.4.434

Overholser, B. R., & Sowinski, K. M. (2008). Biostatistics Primer: Part 2. *Nutrition in Clinical Practice*, *23*(1), 76-84. https://doi.org/https://doi.org/10.1177/011542650802300176

Pan, Q., Feng, W., Wang, R., Tabuchi, A., Li, P., Nitzsche, B.,…Ning, G. (2022). Pulsatility damping in the microcirculation: Basic pattern and modulating factors. *Microvascular Research*, *139*, 104259. https://doi.org/https://doi.org/10.1016/j.mvr.2021.104259

Papaioannou, T. G., & Stefanadis, C. (2005). Vascular wall shear stress: basic principles and methods. *Hellenic J Cardiol*, *46*(1), 9-15.

Perry, B. G., Lucas, S. J. E., Thomas, K. N., Cochrane, D. J., & Mündel, T. (2014). The effect of hypercapnia on static cerebral autoregulation. *Physiological Reports*, *2*(6), e12059. https://doi.org/10.14814/phy2.12059

Pohl, U., Holtz, J., Busse, R., & Bassenge, E. (1986). Crucial role of endothelium in the vasodilator response to increased flow in vivo. *Hypertension*, *8*(1), 37-44. https://doi.org/10.1161/01.hyp.8.1.37

Pott, F., Ray, C. A., Olesen, H. L., Ide, K., & Secher, N. H. (1997). Middle cerebral artery blood velocity, arterial diameter and muscle sympathetic nerve activity during post-exercise muscle ischaemia. *Acta Physiologica Scandinavica*, *160*(1), 43-47. https://doi.org/10.1046/j.1365-201x.1997.00126.x

Prodel, E., Balanos, G. M., Braz, I. D., Nobrega, A. C. L., Vianna, L. C., & Fisher, J. P. (2016). Muscle metaboreflex and cerebral blood flow regulation in humans: implications for exercise with blood flow restriction. *American Journal of Physiology-Heart and Circulatory Physiology*, *310*(9), H1201-H1209. https://doi.org/10.1152/ajpheart.00894.2015

Ras, R. T., Streppel, M. T., Draijer, R., & Zock, P. L. (2013). Flow-mediated dilation and cardiovascular risk prediction: A systematic review with meta-analysis. *International Journal of Cardiology*, *168*(1), 344-351. https://doi.org/https://doi.org/10.1016/j.ijcard.2012.09.047

Ratchford, S. M., Bunsawat, K., Alpenglow, J. K., Zhao, J., Wright, J. B., Ryan, J. J., & Wray, D. W. (2022). Improved vascular function and functional capacity following l-citrulline administration in patients with heart failure with preserved ejection fraction: a single-arm, open-label, prospective pilot study. *Journal of Applied Physiology*, *134*(2), 328-338. https://doi.org/10.1152/japplphysiol.00445.2022

Raven, P. B. (2008). Recent Advances in Baroreflex Control of Blood Pressure during Exercise in Humans: An Overview. *Medicine & Science in Sports & Exercise*, *40*(12).

Reed, K. S., Frescoln, A. M., Keleher, Q., Brellenthin, A. G., Kohut, M. L., & Lefferts, W. K. (2024). Effects of aerobic exercise training on cerebral pulsatile hemodynamics in middle-aged adults with elevated blood pressure/stage 1 hypertension. *Journal of Applied Physiology*, *136*(6), 1376-1387. https://doi.org/10.1152/japplphysiol.00689.2023

Reivich, M. (1964). Arterial Pco2 and cerebral hemodynamics. *American Journal of Physiology-Legacy Content*, *206*(1), 25-35. https://doi.org/10.1152/ajplegacy.1964.206.1.25

Reymond, P., Westerhof, N., & Stergiopulos, N. (2012). Systolic Hypertension Mechanisms: Effect of Global and Local Proximal Aorta Stiffening on Pulse Pressure. *Annals of Biomedical Engineering*, *40*(3), 742-749. https://doi.org/10.1007/s10439-011-0443-x

Robbins, P. A., Conway, J., Cunningham, D. A., Khamnei, S., & Paterson, D. J. (1990). A comparison of indirect methods for continuous estimation of arterial PCO2 in men. *J Appl Physiol (1985)*, *68*(4), 1727-1731. https://doi.org/10.1152/jappl.1990.68.4.1727

Rotto, D. M., & Kaufman, M. P. (1988). Effect of metabolic products of muscular contraction on discharge of group III and IV afferents. *Journal of Applied Physiology*, *64*(6), 2306-2313. https://doi.org/10.1152/jappl.1988.64.6.2306

Rotto, D. M., Stebbins, C. L., & Kaufman, M. P. (1989). Reflex cardiovascular and ventilatory responses to increasing H+ activity in cat hindlimb muscle. *Journal of Applied Physiology*, *67*(1), 256-263. https://doi.org/10.1152/jappl.1989.67.1.256

Rubanyi, G. M., Romero, J. C., & Vanhoutte, P. M. (1986). Flow-induced release of endothelium-derived relaxing factor. *American Journal of Physiology-Heart and Circulatory Physiology*, *250*(6), H1145-H1149. https://doi.org/10.1152/ajpheart.1986.250.6.H1145

Ruediger, S. L., Koep, J. L., Keating, S. E., Pizzey, F. K., Coombes, J. S., & Bailey, T. G. (2021). Effect of menopause on cerebral artery blood flow velocity and cerebrovascular reactivity: Systematic review and meta-analysis. *Maturitas*, *148*, 24-32. https://doi.org/10.1016/j.maturitas.2021.04.004

Ruediger, S. L., Pizzey, F. K., Koep, J. L., Coombes, J. S., Askew, C. D., & Bailey, T. G. (2023). Comparison of peripheral and cerebral vascular function between premenopausal, early

and late postmenopausal females. *Experimental Physiology*, *108*(3), 518-530. https://doi.org/https://doi.org/10.1113/EP090813

Rybicki, K. J., Kaufman, M. P., Kenyon, J. L., & Mitchell, J. H. (1984). Arterial pressure responses to increasing interstitial potassium in hindlimb muscle of dogs. *American Journal of Physiology-Regulatory, Integrative and Comparative Physiology*, *247*(4), R717-R721. https://doi.org/10.1152/ajpregu.1984.247.4.R717

Salam, A. M. (2019). The Invention of Electrocardiography Machine. *Heart Views*, *20*(4), 181-183. https://doi.org/10.4103/heartviews.heartviews_102_19

Sausen, M. T., Delaney, E. P., Stillabower, M. E., & Farquhar, W. B. (2009). Enhanced metaboreflex sensitivity in hypertensive humans. *EUROPEAN JOURNAL OF APPLIED PHYSIOLOGY*, *105*(3), 351-356. https://doi.org/10.1007/s00421-008-0910-8

Sinoway, L. I., Hendrickson, C., Davidson, W. R., Prophet, S., & Zelis, R. (1989). Characteristics of flow-mediated brachial artery vasodilation in human subjects. *Circulation Research*, *64*(1), 32-42. https://doi.org/10.1161/01.res.64.1.32

Sinoway, L. I., Smith, M. B., Enders, B., Leuenberger, U., Dzwonczyk, T., Gray, K.,…Moore, R. L. (1994). Role of diprotonated phosphate in evoking muscle reflex responses in cats and humans. *American Journal of Physiology-Heart and Circulatory Physiology*, *267*(2), H770-H778. https://doi.org/10.1152/ajpheart.1994.267.2.H770

Smith, K. J., Hoiland, R. L., Grove, R., Mckirdy, H., Naylor, L., Ainslie, P. N., & Green, D. J. (2019). Matched increases in cerebral artery shear stress, irrespective of stimulus, induce similar changes in extra-cranial arterial diameter in humans. *Journal of Cerebral Blood Flow & Metabolism*, *39*(5), 849-858. https://doi.org/10.1177/0271678x17739220

Smith, K. J., MacLeod, D., Willie, C. K., Lewis, N. C., Hoiland, R. L., Ikeda, K.,…Ainslie, P. N. (2014). Influence of high altitude on cerebral blood flow and fuel utilization during exercise and recovery. *J Physiol*, *592*(24), 5507-5527. https://doi.org/10.1113/jphysiol.2014.281212

Stebbins, C. L., & Longhurst, J. C. (1985). Bradykinin-induced chemoreflexes from skeletal muscle: implications for the exercise reflex. *Journal of Applied Physiology*, *59*(1), 56-63. https://doi.org/10.1152/jappl.1985.59.1.56

Tarumi, T., Ayaz Khan, M., Liu, J., Tseng, B. Y., Parker, R., Riley, J.,…Zhang, R. (2014). Cerebral hemodynamics in normal aging: central artery stiffness, wave reflection, and pressure pulsatility. *J Cereb Blood Flow Metab*, *34*(6), 971-978. https://doi.org/10.1038/jcbfm.2014.44

Teixeira, A. L., & Vianna, L. C. (2022). The exercise pressor reflex: An update. *Clinical Autonomic Research*, *32*(4), 271-290. https://doi.org/10.1007/s10286-022-00872-3

Thijssen, D. H., Black, M. A., Pyke, K. E., Padilla, J., Atkinson, G., Harris, R. A.,…Green, D. J. (2011). Assessment of flow-mediated dilation in humans: a methodological and physiological guideline. *Am J Physiol Heart Circ Physiol*, *300*(1), H2-12. https://doi.org/10.1152/ajpheart.00471.2010

Thijssen, D. H. J., Bruno, R. M., Van Mil, A. C. C. M., Holder, S. M., Faita, F., Greyling, A.,…Ghiadoni, L. (2019). Expert consensus and evidence-based recommendations for the assessment of flow-mediated dilation in humans. *European Heart Journal*, *40*(30), 2534-2547. https://doi.org/10.1093/eurheartj/ehz350

Thomas, H. J., Marsh, C. E., Naylor, L. H., Ainslie, P. N., Smith, K. J., Carter, H. H., & Green, D. J. (2021). Resistance, but not endurance exercise training, induces changes in

cerebrovascular function in healthy young subjects. *American Journal of Physiology-Heart and Circulatory Physiology*, *321*(5), H881-H892. https://doi.org/10.1152/ajpheart.00230.2021

Thomas, K. N., Lewis, N. C., Hill, B. G., & Ainslie, P. N. (2015). Technical recommendations for the use of carotid duplex ultrasound for the assessment of extracranial blood flow. *Am J Physiol Regul Integr Comp Physiol*, *309*(7), R707-720. https://doi.org/10.1152/ajpregu.00211.2015

Thurston, T. S., Weavil, J. C., Georgescu, V. P., Wan, H. Y., Birgenheier, N. M., Morrissey, C. K.,…Amann, M. (2023). The exercise pressor reflex - a pressure-raising mechanism with a limited role in regulating leg perfusion during locomotion in young healthy men. *J Physiol*, *601*(20), 4557-4572. https://doi.org/10.1113/jp284870

Toda, N. (2012). Age-related changes in endothelial function and blood flow regulation. *Pharmacol Ther*, *133*(2), 159-176. https://doi.org/10.1016/j.pharmthera.2011.10.004

Toth, P., Tarantini, S., Csiszar, A., & Ungvari, Z. (2017). Functional vascular contributions to cognitive impairment and dementia: mechanisms and consequences of cerebral autoregulatory dysfunction, endothelial impairment, and neurovascular uncoupling in aging. *American Journal of Physiology-Heart and Circulatory Physiology*, *312*(1), H1-H20. https://doi.org/10.1152/ajpheart.00581.2016

Trinity, J. D., Wray, D. W., Witman, M. A., Layec, G., Barrett-O'Keefe, Z., Ives, S. J.,…Richardson, R. S. (2016). Ascorbic acid improves brachial artery vasodilation during progressive handgrip exercise in the elderly through a nitric oxide-mediated mechanism. *Am J Physiol Heart Circ Physiol*, *310*(6), H765-774. https://doi.org/10.1152/ajpheart.00817.2015

Tymko, M. M., Drapeau, A., Vieira-Coelho, M. A., Labrecque, L., Imhoff, S., Coombs, G. B.,…Brassard, P. (2024). Acute isometric and dynamic exercise do not alter cerebral sympathetic nerve activity in healthy humans. *Journal of Cerebral Blood Flow & Metabolism*. https://doi.org/10.1177/0271678x241248228

Tymko, M. M., Hoiland, R. L., Kuca, T., Boulet, L. M., Tremblay, J. C., Pinske, B. K.,…Foster, G. E. (2016). Measuring the human ventilatory and cerebral blood flow response to CO2: a technical consideration for the end-tidal-to-arterial gas gradient. *Journal of Applied Physiology*, *120*(2), 282-296. https://doi.org/10.1152/japplphysiol.00787.2015

Underwood, D. (2024). *Mechanisms of cerebral artery compliance at sea-level and following acclimatization to high altitude.* University of Victoria. https://hdl.handle.net/1828/16356

van den Kerkhof, M., van der Thiel, M. M., van Oostenbrugge, R. J., Postma, A. A., Kroon, A. A., Backes, W. H., & Jansen, J. F. (2023). Impaired damping of cerebral blood flow velocity pulsatility is associated with the number of perivascular spaces as measured with 7T MRI. *J Cereb Blood Flow Metab*, 271678x231153374. https://doi.org/10.1177/0271678x231153374

Verbree, J., Bronzwaer, A., van Buchem, M. A., Daemen, M., van Lieshout, J. J., & van Osch, M. (2017). Middle cerebral artery diameter changes during rhythmic handgrip exercise in humans. *J Cereb Blood Flow Metab*, *37*(8), 2921-2927. https://doi.org/10.1177/0271678x16679419

Wan, H. Y., Weavil, J. C., Thurston, T. S., Georgescu, V. P., Bledsoe, A. D., Jessop, J. E.,…Amann, M. (2020). The muscle reflex and chemoreflex interaction: ventilatory implications for the exercising human. *J Appl Physiol (1985)*, *129*(4), 691-700. https://doi.org/10.1152/japplphysiol.00449.2020

Washio, T., Suzuki, K., Saito, S., Watanabe, H., Ando, S., Brothers, R. M., & Ogoh, S. (2021). Effects of acute interval handgrip exercise on cognitive performance. *Physiology & Behaviour*, *232*, Article 113327. https://doi.org/10.1016/j.physbeh.2021.113327

West, J. B. (1971). Causes of carbon dioxide retention in lung disease. *N Engl J Med*, *284*(22), 1232-1236. https://doi.org/10.1056/nejm197106032842202

Williamson, J. W. (2010). The relevance of central command for the neural cardiovascular control of exercise. *Experimental Physiology*, *95*(11), 1043-1048. https://doi.org/10.1113/expphysiol.2009.051870

Willie, C. K., Colino, F. L., Bailey, D. M., Tzeng, Y. C., Binsted, G., Jones, L. W.,…Ainslie, P. N. (2011). Utility of transcranial Doppler ultrasound for the integrative assessment of cerebrovascular function. *J Neurosci Methods*, *196*(2), 221-237. https://doi.org/10.1016/j.jneumeth.2011.01.011

Willie, C. K., Macleod, D. B., Shaw, A. D., Smith, K. J., Tzeng, Y. C., Eves, N. D.,…Ainslie, P. N. (2012). Regional brain blood flow in man during acute changes in arterial blood gases. *J Physiol*, *590*(14), 3261-3275. https://doi.org/10.1113/jphysiol.2012.228551

Woodman, R. J., Playford, D. A., Watts, G. F., Cheetham, C., Reed, C., Taylor, R. R.,…Green, D. (2001). Improved analysis of brachial artery ultrasound using a novel edge-detection software system. *J Appl Physiol (1985)*, *91*(2), 929-937. https://doi.org/10.1152/jappl.2001.91.2.929

World Health Organization. (2024). *Brain Health*. Retrieved from https://www.who.int/health-topics/brain-health#tab=tab_1

Yoon, J. H., Lee, J. S., Yong, S. W., Hong, J. M., & Lee, P. H. (2014). Endothelial dysfunction and hyperhomocysteinemia in Parkinson's disease: Flow-mediated dilation study. *Movement Disorders*, *29*(12), 1551-1555. https://doi.org/10.1002/mds.26005

Appendix A. Adjusted MAP Values

Participant #	BL Breathing Test MAP (mmHg)	BL PEMI Test MAP (mmHg)	Resting MAP from Automatic Cuff (mmHg)	Abs. MAP Change Breathing Test (±mmHg)	Abs. MAP Change PEMI Test (±mmHg)
1	77.93	84.94	91.33	11.44	5.95
2	69.98	69.68	89.33	15.16	15.33
3	90.74	91.85	92.00	1.24	0.15
4	85.58	89.83	85.00	-0.58	-5.10
5	66.60	58.10	94.00	19.41	22.19
6	68.15	73.30	90.33	16.74	13.82
7	60.42	83.23	95.33	22.13	10.57
8	58.55	52.66	93.00	21.69	22.84
9	70.65	96.93	91.33	16.00	-5.94
10	71.00	61.95	80.33	8.25	14.18
11	65.73	66.74	77.00	9.62	8.89
12	70.82	75.44	84.67	11.58	8.22
13	70.24	73.63	86.67	13.31	11.08
14	70.32	80.36	90.67	15.78	9.14
16	113.35	139.70	101.00	-13.86	-53.53
17	65.90	73.51	92.33	18.87	14.99
18	92.15	92.28	88.33	-3.98	-4.12
19	56.26	70.92	90.33	21.22	15.24
20	72.53	77.83	81.33	7.85	3.35
21	77.44	65.79	84.67	6.61	14.67
22	100.52	104.74	96.00	-4.73	-9.53
23	96.01	108.57	91.33	-4.92	-20.48
24	76.27	78.06	89.00	10.91	9.60
25	53.79	65.60	102.00	25.42	23.41
26	75.57	78.56	103.33	20.31	18.84
27	90.35	99.95	84.67	-6.06	-18.04
28	97.34	95.32	90.67	-7.16	-4.89

Table A.1. Detailed baseline/resting MAP values and calculated change values, which were applied to the MAP datasets for both the breathing test and PEMI test; these data transforms were standardized and based on individual participant resting data. Note a missing participant #15, due to attrition.

Appendix B. Example Scripts for RStudio

Within these scripts, “EF” refers to hypercapnic breathing test, “METAB” refers to the handgrip with subsequent PEMI, and “MF” refers to male-female comparisons; “MEASURE”, “UNITS”, and “PARTICIPANT” are placeholders that refer to any specific measured outcome during the testing with their units and the specific participant ID, respectively.

```
➔ pacman::p_load(ggplot2, tidyr, dplyr, magrittr, tidyverse, ggpubr, rstatix, nlme, lme4,
  extrafont, Hmisc, ggcorrplot, reshape2, gcplyr, pROC, DescTools, pwr, pwrss)

  #Z-scores

➔ z_scores <- (MEASURE_EF$UNITS -
  mean(MEASURE_EF$UNITS))/sd(MEASURE_EF$UNITS)
➔ MEASURE_EF <- MEASURE_EF %>% mutate(z_scores)
➔ z_scores <- (MEASURE_METAB$UNITS -
  mean(MEASURE_METAB$UNITS))/sd(MEASURE_METAB$UNITS)
➔ MEASURE_METAB <- MEASURE_METAB %>% mutate(z_scores)

  #One-Way ANOVA

➔ bartlett.test(UNITS ~ Stages, data = MEASURE_EF)
➔ MEASURE_EF %>%
    group_by(Stages) %>%
    shapiro_test(UNITS)
➔ res.aov <- anova_test(data = MEASURE_EF, dv = UNITS, wid = P, within = Stages)
  get_anova_table(res.aov)
➔ pwc <- MEASURE_EF %>%
    pairwise_t_test(UNITS ~ Stages, paired = TRUE, p.adjust.method = "bonferroni")
  pwc
➔ bartlett.test(UNITS ~ Stages, data = MEASURE_METAB)
➔ MEASURE_METAB %>%
    group_by(Stages) %>%
    shapiro_test(UNITS)
➔ res.aov <- anova_test(data = MEASURE_METAB, dv = UNITS, wid = P, within =
  Stages)
  get_anova_table(res.aov)
➔ pwc <- MEASURE_METAB %>%
    pairwise_t_test(UNITS ~ Stages, paired = TRUE, p.adjust.method = "bonferroni")
  pwc
➔ print(pwc, n = 45)

  #Kruskal-Wallis

➔ res.kruskal <- MEASURE_EF %>% kruskal_test(UNITS ~ Stages)
  res.kruskal
```

```
➔ MEASURE_EF %>% kruskal_effsize(UNITS ~ Stages)
➔ pwc <- MEASURE_EF %>%
    dunn_test(UNITS ~ Stages, p.adjust.method = "bonferroni")
  pwc
➔ res.kruskal <- MEASURE_METAB %>% kruskal_test(UNITS ~ Stages)
  res.kruskal
➔ MEASURE_METAB %>% kruskal_effsize(UNITS ~ Stages)
➔ pwc <- MEASURE_METAB %>%
    dunn_test(UNITS ~ Stages, p.adjust.method = "bonferroni")
  pwc
➔ print(pwc, n = 45)

  #Correlations
➔ ggscatter(MEASURE1_ MEASURE2_EF, x = "UNITS1", y = "UNITS2",
    add = "reg.line", conf.int = TRUE, cor.coef = TRUE, cor.method = "pearson", xlab =
  "UNITS1", ylab = "UNITS2") +
      theme(text = element_text(size = 16,  family = "serif"),
          axis.line = element_line('black', size = 0.5),
          panel.grid.major = element_blank(),
          panel.grid.minor = element_blank(),
          panel.border = element_blank(),
          panel.background = element_blank())

  #Shear Rate AUC

➔ AUC(x = Stages, y = PARTICIPANT$Rate, from = min(120, na.rm = TRUE), to =
  max((T2P+120), na.rm = TRUE), method = c("step"), absolutearea = FALSE, na.rm =
  FALSE)

  #Change Scores

➔ MEASURE_EF_CHG %>%
    group_by(Comps) %>%
    summarise(UNITS_median = median(UNITS), UNITS_IQR = IQR(UNITS))
➔ MEASURE_METAB_CHG %>%
    group_by(Comps) %>%
    summarise(UNITS_median = median(UNITS), UNITS_IQR = IQR(UNITS))

  #Sex-Comparisons

➔ res.kruskal <- MEASURE_MF %>% kruskal_test(Males*Females ~ Stages)
  res.kruskal
➔ MEASURE_MF %>% kruskal_effsize(Males*Females ~ Stages)
➔ pwc <- MEASURE_MF %>%
    dunn_test(Males ~ Stages, p.adjust.method = "bonferroni")
  pwc
```

```
➔ pwc <- MEASURE_MF %>%
    dunn_test(Females ~ Stages, p.adjust.method = "bonferroni")
  pwc
➔ MEASURE_MF %>%
    group_by(Stages) %>%
    summarise(Males_median = median(Males), Females_median = median(Females))
```